Response to reviewer comments for manuscript: "Composition and volatility of SOA formed from oxidation of real tree emissions compared to ~~simple~~ simplified VOC-systems"

Ylisirniö et. al

We thank the two reviewers for their constructive comments regarding the paper. Below we address the specific issues point by point. The reviewer's comments are in black and our answers are in blue. Changes to the Manuscript or Supplement Information are highlighted in red.
Line numbers before the red response text refer to line numbers in the modified manuscript.

Additional changes by authors:

Due to graphing mistake, all C* values shown in Figures 6-8 were one order of magnitude too high. These figures have been redrawn with correct values. As this change is in all experiments, our conclusions from the figures stay the same.

The language of the text is also slightly adjusted for better readability.

Reviewer 1:

Major comments:

l. 25: Bisabolenes also have endocyclic double bonds. Their oxidation would not lead to smaller and more volatile compounds. I suggest rephrasing to "[...] is due to exocyclic C=C bond scission [...]"

The text was rephrased as suggested.

l. 62: not only mixtures of VOCs influence the composition of products, but also trace gases like NOx and CO. Furthermore, ammonia and H2SO4 can alter particle phase composition through heterogeneous reactions with organic molecules. It would be good to cite a review at this point (e.g. Ng et al., ACP, 2017, doi:10.5194/acp-17-2103-2017 for the NOx effects).

The text was modified as suggested.

l. 82: Was the temperature actually monitored/regulated during the experiments, or does 25◦C just mean that experiments were done in the laboratory? I can imagine that the temperature changes in the flow tube when UV lamps are switched or when UV exposure is modulated.

Both the temperature in the OFR and in the room were monitored during the experiments. The room was air conditioned to ~21 °C. Due to the heat from the UV lamps inside OFR, the temperature in the reactor was at ~26 °C after the initial "warm-up" phase. Then the reaction temperature was stable within +/- 1 °C or less during the experiment. Care was taken to allow sufficient time for the setup to stabilize before collecting the FIGAERO samples.

Section 2.1: A more thorough description of the OFR-experiments is urgently needed. With the current description, it would be impossible to replicate these experiments. Instead of mentioning already results in the methods section (l. 84/85, l. 101), the level of information on the setup in the current version is unsatisfactory. As a reader I like to know for example: How were blank experiments conducted? Was there a carry-over between different experiments when VOC precursors were changed? Did VOCs / SVOCs come back from the wall when switching on UV lamps? What were the flow rates? How were the VOCs flushed into the chamber (material of the tubing?)? Were the source- and sampling-lines heated to avoid condensation of sesquiterpenes?...

We extended the setup description in section 2.1 (including a reference to an earlier study with similar setup (Buchholz et al. 2019)) to the following:

Line 82 onwards:

We conducted experiments with SOA generated from the ozonolysis and photo-oxidation of VOCs by hydroxyl radicals (OH) in a Potential Aerosol Mass (PAM) OFR (Kang et al., 2007; Lambe et al., 2011) in the absence of seed particles. The experimental setup is similar to that in our previous study (Buchholz et al., 2019). A schematic of the setup is shown in Figure 1 and all experimental conditions are listed in Table 1 and Table 2. We provide a very brief description of the experimental setup here and more detailed information can be found in the SI material (Sect. S2). A flow containing 200 to 400 ppb of the investigated VOCs was mixed with an O_3 containing flow directly before entering the OFR. With

two UV lamps (254 nm), O_3 was photolyzed to O (1D) which reacted with water vapor to produce OH radicals. A wide range of OH exposure was achieved by adjusting the voltage of 254-nm UV lamps in the OFR and changing the O_3 concentration. Overall, the integrated OH exposure in the OFR ranged from approx. 6.6×10^{10} to 2.5×10^{12} molec cm^{-3} s across all experiments as calculated according to methods described by Peng et al., (2015, 2016). This range of OH exposure corresponds to 0.5 to 19 equivalent days of atmospheric aging at an OH concentration of 1.5×10^{6} molec cm^{-3} (Palm et al., 2016). In all experiments, the operation temperature of the OFR was 25 or 27 ˚C and relative humidity (RH) was between 40% and 60%. For the Scots pine experiments, VOCs were introduced by flushing purified air through a plant enclosure (Tedlar®) containing a 6-year-old Scots pine sapling. In the α-pinene (Sigma Aldrich, 98 % purity) and sesquiterpene mix (mixture of acyclic/monocyclic sesquiterpenes, Sigma Aldrich) experiments, the VOC's were introduced into a flow of clean N_2 by using a diffusion source or a dynamic dilution system (Kari et al., 2018). For the Scots pine experiment 4, the plant was injured by making four 0.5-1 cm^2 cuts into the bark of the plant exposing resin pools and thus increasing the VOC emissions.

We also added a more detailed description of the OFR experiments in the supplement material sect. S2:

Line 15 in SI:

SOA was generated by oxidizing different VOCs by OH radicals and O_3 in the OFR, in the absence of seed particles. VOCs were introduced by flushing clean air/N_2 through different sources. For the Scots pine experiments, VOCs were introduced by flushing purified air through a plant enclosure containing a 6-year-old Scots pine sapling. For α-pinene and sesquiterpenes SOA experiments, VOC vapors were introduced into a flow of dry N_2 using a diffusion source or a dynamic dilution system (Kari et al., 2018). In the dynamic dilution system, a set volume of VOCs was continuously injected into a heated N_2 flow with a syringe pump. The VOC-containing flow was then mixed with other make-up flows before entering the OFR. To achieve the desired RH, water vapor was introduced by passing a flow of N_2 through a Nafion humidifier (Model FC100-80-6MSS, Perma Pure). O_3 was generated in an external generator by irradiating a flow of O_2 or purified air with a 185-nm UV lamp. The exact ratios of these flows (VOC-, O_3, and humidified flow) varied between the different sets of experiments. But all relevant parameters of the mixture entering the OFR were carefully monitored. The mixing ratio of VOCs was continuously measured by a proton transfer reaction time-of-flight mass spectrometer (PTR-MS, PTR-TOF 8000, Ionicon Analytik, Austria) before mixing with O_3. To minimize line losses, the combined PFA (~2.5m, 6 mm outer diameter) and PEEK (~1 m, 1/16'' outer diameter) sampling line to the PRT-MS was heated to 60 °C. All other sampling lines were unheated stainless steel or conductive silicon tubing (Tygon®) as this work was focused on the particle phase composition. Overall, 2.5 or 5 L

min^{-1} of mixed flow containing 200 - 400 ppb of VOCs was introduced into the OFR for photooxidation and ozonolysis, with leads to residence times in the OFR ranging from 120 to 300 s (assuming plug flow).

Inside the OFR, $O(^1D)$ was generated from the photolysis of O_3 with 254 nm lamps and reacted with water vapor to form OH radicals. To minimize the impact of heat generated from the 254-nm lamps, we continuously purged the lamps with N_2. We varied the OH exposure by adjusting the voltage of the 254-nm lamps inside the OFR and/or the ingoing O_3 concentration. The resulting OH exposure ranged from approx. 6.6×10^{10} to 2.5×10^{12} molec cm^{-3} s in the OFR, using the model calculations described by Peng et al. (2015, 2016) taking the external OH reactivity into account. Assuming an ambient OH concentration of 1.5×10^{6} molec cm^{-3}, this range of OH exposure corresponds to 0.5 to 19 equivalent days of atmospheric aging. Before and after each SOA experiment, we always conduced photooxidation cleaning for the OFR for several hours, i.e. flushing the PAM reactor with the same flows as during the experiments but without adding any VOCs. Background particle number concentration decreased to less than 2,000 # cm^{-3}, (particle mass < 0.1 µg m^{-3}. These values were neglectable in comparison to the 10^6 – 10^8 particles # cm^{-3} (and 50 – 500 µg m^{-3}) which were formed during the experiments. After the photooxidation cleaning, the VOC concentrations detected with the PTR-MS were within the instrument background. Care was taken to allow sufficient time after the VOC type or concentrations was changed.

l. 107: What does the different "use history" of the PAM chambers mean? That statement leaves the reader questioning whether the history of experiments has an effect on the results?

As laid out in our reply to the previous comment, great care was taken to clean the PAM reactor and all connected lines between experiments, especially when the VOC type was changed.
With the term "usage history" we wanted to refer to the fact that while "PAM1" had been in use for a long time and the UV lamps were getting close to the end of their lifetime, "PAM2" was brand new. This together with other experimental constrains (e.g. sampling flow requirements for instrumentation) led to a different combination of light intensity, residence time, and O_3 concentration needed to replicate the OH exposure range and oxidation state of the formed SOA particles.
As the term "usage history" clearly lead to some confusion, we have removed it and rephrased the sentence:

Line 115:

For a detailed description of the mixture see Table S1 and Fig. S1. For those follow-up experiments, a nominally identical OFR was used ("PAM 2"). However, to recreate the same OH exposure and particle composition (as characterised by particle oxidation ratio, see below) a different combination of light intensity, residence time, and O3 concentration was necessary in the follow-up experiments. Thus, the results are presented separately and marked PAM1 or PAM2.

Section 2.2: The level of experimental detail is unsatisfactory. A "suite of instruments" is mentioned in l. 112-115, but the following paragraphs only describe FIGAERO-CIMS and nothing on AMS or SMPS measurements. Concerning AMS, more information is needed in this experimental part, e.g. on the version (HR-AMS or C-ToF), operation mode (V-mode or W-mode) of the AMS, with/without size dependent composition, etc. Furthermore, key information of FIGAERO-CIMS operation mode are also missing: how were blank measurements conducted? Have the authors evaluated whether gas-phase adsorption on the particle filter can be an issue? What was the sample flow rate and the duration of particle collection? Until which maximum desorption temperature the ramp was operated? What was the pressure in the ion molecular region? etc.

More information about the instruments and methods have been added to section 2.2. However, as this study focuses on the particle composition derived from FIGAERO-CIMS measurements, we added the requested additional information about other instruments into the supplement material Sect. S4:

Line 125:

AMS and SMPS were used to continuously monitor the output SOA particle mass and size distribution from the OFR to determine the point when the particle concentrations and distributions had stabilized for a given OFR condition. Then the filter collection for FIGAERO-CIMS was started, so that only steady-state SOA was sampled. More information about these other instruments is given in Sect. S4.

Line 53 in SI:

S4 SOA characterisation

The outflow of the OFR was periodically checked with the PTR-MS to ensure that our assumption of complete consumption of the ingoing VOCs was correct. The same 2.5 m (outer diameter 6 mm) PFA + 1 m (outer diameter 1/16'') PEEK line heated to 60 °C was used for sampling before or after the OFR. When the sampling point was changed sampling lasted at least 30 min to ensure all compounds had reached their final values (especially sesquiterpenes).

The outflow of the OFR was continuously monitored with an AMS and a SMPS. The SMPS was operated with a closed loop sheath flow. The RH and temperature measured in the sheath flow in the instrument was close to the experimental conditions in the OFR.

The AMS was operated in V-mode and although particle size resolved data was collected, only the integrated signal was used for the analysis. The raw data was processed with the SQUIRREL (Version 1.59D) and PIKA toolkits (Version 1.19, Decarlo et al., 2006). As the composition of the "air" in OFR changed depending on the ratio between the N_2 and O_2 flows introduced into it, a time dependent air beam and CO_2 correction was applied. The main purpose of the AMS measurements were to classify the SOA particles by their oxidation state (O:C and H:C ratios, OS_C). The improved parameterisation from Canagaratna et al., 2015 was used to derive these values from the data.

We performed a blank measurement with FIGAERO-CIMS before each measurement to make sure the filter was clean of residual compounds and to determine any instrument artefacts. For our samples, the collection time (i.e. the time the filter was exposed to the sample gas and particle phase was short (~2 minutes) and high mass loading (~500 ng – 1350 ng) were collected. Thus, we can assume that generally signals from gas phase adsorption are minor compared to signal stemming from collected particles. However, in the data-analysis we identified a small group of signals (mostly lactic and formic acid) that were suspected to originate from gas phase adsorption or other additional contamination due to the shape of their thermograms. They all exhibited high signals already at the start of the desorption and a smooth increase with increasing temperature. These signals accounted for around 1% of total signal and were excluded from further analysis.

The blank measurements are now discussed in the text:

Line 154:

A blank measurement, meaning a measurement with no particles collected on the filter, was performed before each measurement to make sure the filter was clean of residual compounds and to determine any instrument artefacts. The assure that filter did not contain any particles, collection flow leading to the filter was shut down between actual measurements. These blank measurements were also considered in the data-analysis. The relatively high collected particle mass loading (between 500 and 1350 ng) on the filter ensured that the majority of the signal came from the evaporating SOA particles, and that the instrument background/artefacts were neglectable. The FIGAERO filter was also visually inspected daily and replaced when needed.

Figaero data analysis: Why did the authors use tofTools and not Tofware, which offers also a figaero-version? Concerning peak identification: What are the numbers of allowed elements for C, H and O? How were multiple possible sum formulas for one exact mass ranked? Were ratios of H/C or O/C and double bound equivalents used to further constrain sum formula?

The reviewer is correct in pointing out that the Tofware software includes a FIGAERO – data-analysis package. However, the post processing of the FIGAERO-CIMS data required heavy use of custom-made analysis scripts, which were done with Matlab. Using tofTools-preprocessing software enabled keeping the whole analysis inside one programming system.

In peak identification, we used upper limits of H/C = 2.5 and O/C = 2 as constraints for possible compositions. These limits constrain the majority of the signal in each experiment. However, there was a small number of signals with mass defects that could only be explained with formulas with higher H/C or O/C value even though such compositions seem unrealistic. These compounds comprised only a small amount of total signal and thus did not impact the reported average formula. We did not use any DBE limits as previous studies (Kourtchev et al., 2014) have shown that possible DBE value increases with molecular mass.

l. 167: Was an experiment conducted to measure wall/sampling line loss rates of sesquiterpenes against monoterpenes? E.g. SQT/MT measurements before and after the OFR, without O3 and UV off?

We did not conduct such measurements but will consider them in future projects to get a more thorough characterization of our OFR.

We followed the recommended procedure for PTR-MS measurements at the time using a PFA or PEEK sampling line heated to 60 °C which minimizes any condensation of SQT or MT in the sampling line. We measured the VOC's 10 cm before the inlet plate of the OFR, which was the closest the PTR-MS measurement inlet could be connected before addition of O_3 to the flow.

As we always utilized large OH exposure levels, and there was ppm level of O_3 in the OFR, the majority of SQT and MT should react with oxidants rapidly after entering the OFR. Thus, we would need to determine the wall loss rates of the products of that oxidation which was far beyond the scope of this study.

L. 171: I disagree with this statement: wall/sampling line losses will be larger for sesquiterpenes than for monoterpenes. Relating this to the observed results, evaluating potential different losses of SQT compared to MT are highly relevant for the conclusions on different SOA yields.

This is a good point. To partly counteract this, we minimized the length of tubing between VOC measurement and inlet of the OFR as much as we could. It is possible that some of the SQTs were lost more than MTs in this short 10 cm tubing and losses in the heated PTR-MS sampling tube could also be different for SQTs and MTs. To address this comment, we rephrased this sentence as follows:

Line 192:
However, because the VOC measurement was made almost immediately before the inlet of the OFR and formed SOA size distribution was roughly identical between different experiments, we assume that possible sampling line wall losses have minor impact on our SOA yield calculations.

Based on Fig. 2: does it need to be reassessed whether a-pinene is the (globally)strongest emitted monoterpene?

We do not believe such a re-assessment is needed. We were looking at the emissions of a single tree at a short time when it was stressed. It is well known that even within one species (here Pinus Sylvestris) there can be many different chemotypes. As an example, there are Pinus Sylvestris trees that emit more Δ-3-carene than a-pinene and those that do not emit this compound at all (Bäck et al. 2012). Also, the time of year plays a major role in the emission patterns (Hakola et al., 2006). This is why global emission inventories are based on a multitude of measurements both directly from branch enclosures and above forest canopies.

Our results highlight that more care must be taken when representing tree emissions in OFR or chamber experiments and that α-pinene is not necessarily representative for all pine forests. These other VOCs (e,g, induced by stressors) may have a significant impact on SOA formation and properties (see also Faiola et al., 2018, 2019)).

l.274-276: this has already been shown by Hall et al.(https://doi.org/10.1021/es303891q)

Thank you for pointing this out. We have added a reference to Hall et. al. 2013.

l. 309-316: Is this observation in line with what one would expect from C* estimates based on the sum formula? (Donahue et al., ACP, 2011). It is surprising that oxygenation outweighs fragmentation of e.g. C20-dimers. Does the VBS distribution look different when the VBS bins are filled based on T_max vs. when they are filled based on the sum-formula-derived volatility?

Sum formula based C* parametrizations tend to yield very different results between different methods (Mohr et al., 2019) and while comparing them to results made with Tmax based C* estimates would be very interesting, it would be outside of the scope of this article. Based on volatility estimations shown in Mohr et al., 2019 measured in boreal forest in Finland, composition based volatility estimations seem to predict higher fraction of volatile compounds classified in SVOC class compared to our results.

Fig. 6 – SQT mix – mass spec: What are the ELVOCs with molecular mass < 200 Da? Are such compounds formed by thermal fragmentation of larger molecules? If this is the case, a quantitative estimate of the fraction of ion signal that results from thermal fragmentation would help to evaluate the FIGAERO mass spectra.

These signals (mass < 200 Da and in the ELVOC region) are C3-C7 compounds with mostly relatively high oxygen content O3-O7. The reviewer is correct when pointing out that they are possibly thermal decomposition products and they comprise about 11% of the total signal.
This is now also pointed out in the text as:

Line 408:
A small number of signals in the sesquiterpene mixture results can confidently be categorized as thermal decomposition products, namely the ones that fall in the ELVOC volatility range, but have relatively small molecular masses (< 200 Da). These compounds are C3-C7 compounds with relatively high oxygen content (O3-O7) and comprise about 11% of the total integrated signal.

l. 418: A comparison FIGAERO spectrum between acyclic and mono/bicyclic SQT would be very interesting. Fig. 4 only shows the spectrum of a SQT mix. More fragmentation products would be expected for the acyclic SQTs.

Such comparison of acyclic vs. mono/bicyclic SQT would be indeed very interesting and would help shed light to some questions raised by our results, and potentially provide additional evidence to the presented hypotheses regarding SQT cyclic structures. Unfortunately, we did not have respectively representative SQT mixtures available at the time of our experiments, so that practical time constraints precluded us from conducting the suggested comparative measurements. We hope that we (or others) will follow up with a thorough investigation of FIGAERO spectra from a variety of SQT in the future.

Minor:

l. 54 add Yassaa et al., ACP, 2012; doi:10.5194/acp-12-7215-2012.

Citation added.

l. 119: oxygen or OH-groups: consider to be more specific. Would an ether (a molecule with an oxygen) already give a stable cluster with iodide?

The reviewer is correct when pointing this out, as mere existence of oxygen in the chemical formula is not enough for this ionization process. Text is changed to:

Line 132:

… clusters with a neutral molecule *M* which contains hydroxy-, hydroperoxy-, carboxyl- or peroxycarboxyl-groups in their structure.

l. 409: Explaining what fragmentation means should not appear in the summary /conclusions.

The reviewer is correct and following lines have been removed, as they have been already discussed in section 3.2.

Line 447:

"When such acyclic compounds are oxidized, the initial reaction with OH or O_3 already leads to fragmentation (i.e. reaction products with much shorter C chain), whereas cyclic compounds, such as many monoterpenes, (including α-pinene and β-phellandrene) but also bicyclic sesquiterpenes (such as β-caryophyllene), generally go through more steps of oxidation before the onset of significant fragmentation is observed."

Technical:

l. 52 replace a-pinene with α-pinene.

Fixed the text.

l. 62, l. 269 replace Mcfiggans with McFiggans.

Fixed the references.

Fig. 2: structural formula of farnesene expliciltly shows one hydrogen. Either draw all hydrogens or none (preferably none),

Figure modified so that no hydrogens are shown in the structure.

Reviewer 2:

Major comments:

Line 26. “SOA particles from the oxidation of Scots pine emission had similar or lower volatility than SOA particles formed from either of single precursor.” Does the single precursors refer to the SQT mixture as well as the alpha pinene? If so that might need rephrasing. This is also true for the title.

Line 28:
Text rephrased as “…SOA particles formed from either single precursor or simple mixture of VOCs.”

Title is rephrased as “Composition and volatility of SOA formed from oxidation of real tree emissions compared to simplified VOC-systems”.

Line 30. You state “These results emphasize that simple increase or decrease of relative monoterpene and sesquiterpene emissions should not be used as indicator of SOA particle volatility” but on line 27 you state “Applying physical stress to the Scotspine plants increased monoterpene emissions, which further decreased SOA particle volatility and increased SOA mass yield.” Can you clarify or rephrase the statement online 30 based on the statement from line 27.

Statement is meant to highlight that change of total monoterpene or sesquiterpene emissions without stating the structures of these compounds should not be used as indicator for SOA properties. Text has been modified to emphasize this.

Line 87. Could you please provide a brief description on the dynamic dilution system you use to mix your VOCs.

The dynamic dilution system has been extensively described in earlier publication by Kari et al. 2018 (Int. Journ. of Mass Spectrometry). The reference is added to the setup description.
Briefly, we use a syringe pump to continuously inject a VOC (or VOC mixture) into a nitrogen flow heated to 35 – 60 °C. A portion of this flow was than mixed with the other flows going to the OFR.

Section 2.2.1/S3 There is some missing information that would be useful. Can you please state the resolution of the ToF-CIMS. A description of your FIGAERO back-grounding methodology and how you account for backgrounds in your analysis is missing. Also a description of your gas and particle sample lines to the ToF-CIMS (material, length, residence time etc).

As Reviewer #1 also requested more detailed information about the setup in general, we extended the methods section and added the more specific details into the supplement material. Please refer to our response to Reviewer #1 above.

Line 169. Although you did not correct for wall losses, can you make an estimation or assessment of their importance? This may be important if the yields from this paper are compared with other experiments.

Directly determining the wall losses of just the main reaction products of α-pinene would be a project on its own. Instead we inspected the model calculations by Palm et al., 2016. They determined the fate of LVOCs in a PAM OFR in relation to the OH exposure. The residence time in their system was comparable to ours, but they were focusing on oxidizing ambient air samples. LVOCs are used as a proxy for condensable vapors/ vapors contributing to SOA formation and growth in the OFR. They estimate that in the absence of any particles, 30% of the LVOC vapors would condense on the OFR walls and the rest would be further oxidized or leave the OFR and potentially condense on tubing surfaces etc. Fig. 5 in Palm et al. (2016) can be used for a qualitative assessment of wall losses once SOA particles are formed in our experiments. Quickly, the “high Condensational Sink” conditions are met, meaning that for our OH exposure range < 15% of LVOC vapours are lost to the OFR walls. Thus, the SOA yields would be underestimated by a similar amount due to LVOC wall losses.

The dynamics of the particle formation will play an important role as we did not use seed particles in these experiments. A more detailed model description of the flow dynamics and chemistry in the OFR would be needed to understand the impact of the different VOC precursors and the different flow setup on the wall losses.

These potential differences in the losses of particles and gaseous compounds is one of the reasons we present results from PAM 1 and PAM 2 setup separately. The different residence times and OH distribution may lead to different losses.

Line 186. Can you provide some more detail on the scrubber / filter for the compressed air.

We used a custom build air purifying unit consisting of a sequence of scrubbers with active charcoal, potassium permanganate and filters to dry the compressed air and clean out any VOCs.

Line 190. Can you provide more information on the LED lamps.

The LED lamps were chosen to create a Photosynthetically Active Radiation (PAR) value similar to that experienced by plants in the Finnish environment. This is now also stated in the text.

Line 210. Is the stress response induced by cutting the sapling reduced or altered because it is already stressed by the infestation? Are there any further considerations required as to how these two stresses alter VOC emission regarding the conclusions you can draw?

The effect of cutting the bark of Scots Pine seedlings is comparable to the damage induced by infestation with bark borers. The main impact on the plant is the exposure of resin pools in the stem (Faiola et al. 2018, Kari et al 2019). As the content of the resin pools is dominated by the longer-term storage and not the immediate production of the infested plant, it can be assumed that the interaction of these two stressors has a very small impact on the emission profiles.

Line 214. Is it shown that MT concentrations were higher? Experiment 2 shows the highest [MT] concentration (table 1). Do you mean the transition from experiment 3 to experiment 4 specifically?

Monoterpene emissions increased from to cutting the sapling by about doubling the monoterpene concentration once the concentrations had stabilized compared to pre-cutting concentrations. This has been clarified in the text as:

Line 237:
"The wounds exposed plants resin pools in the stem and increased the measured monoterpene concentrations compared to pre-cutting concentrations by roughly doubling them."

Line 227. "...are about 30% larger, even though SQT/MT was substantially smaller than in experiments 1-3." I find the words 'even though' confusing, can you explain why these findings are unexpected?

Thank you for pointing this out. The surprise in question stems from results reported earlier by Faiola et. al. 2018 who measured positive correlation with SOA yield and SQT/MT ratio, when they measured SOA formed from VOC's emitted by Scots pine seedlings in similar flow tube experiments as ours. The text has been modified to point out this detail and its then discussed in more detail later in the text.

Line 251:
Earlier study by (Faiola et al., 2018) reported a positive correlation with SOA yield and SQT/MT ratio of VOC's measured from Scots pine seedlings in a flow tube experiment similar to our study.

Line 241. "We conclude that the increase in SOA yield in the Scots pine experiment 4, compared to the Scots pine experiments 1-3, is likely due to the large relative increase in emitted monoterpenes" I think more clarification is needed regarding this conclusion. Can you provide a concise explanation of which factors regarding the MT are important for the increased SOA yield in experiment 4, such as absolute [MT] increase induced by cutting; MT composition change induced by cutting e.g.β-phellandrene to α-pinene ratio; and the SQT/MT ratio (for suppression).

The absolute MT concentration first increased by several orders of magnitude and then stabilized to about 2x the MT concentration before the cutting, as stated in previous comment. Even though the absolute MT concentration in Scots pine experiment 4 is not substantially higher than in Scots pine experiment 3 (127 ppb in exp. 3 vs. 150 ppb in exp. 4), the amount of SQT's are noticeably lower (151 ppb in exp. 3 vs 66 ppb in exp. 4). As we discuss at the end of section 3.2, what most strikingly influences the amount of SOA production is the structure of each VOC compound, in general regardless of its classification as MT or SQT. We believe that concentration of all MTs increased as a result of the tree being cut, but unfortunately there is no GC-data available immediately before and after the cut.

Line 327. "We suggest that the increased desorption temperatures for the Scots pine experiments 1-3 relative to the α-pinene experiment" Do you mean from exps 1 – 3 you see an increase in Tmax and this is explained by increasing contributions of farnesenes? Or that farnesene concentrations are broadly the same for exps 1 – 3 and have the same (broad) Tmax? Is this why there are only 2 Tmaxes shown on figure 5b, rather than 4?

Scots pine experiments 1-3 were broadly similar to each other in terms of desorption behavior and VOC concentrations, which is indeed why they are compared to Scots pine experiment 4 as a group and why only 2 Tmaxes are shown in Figure 5b). As the Tmax values of Scots pine experiments 1-3 are also quite close to each other, only Tmax values from Scots pine exp. 1 and Scots pine exp.4 are shown in the Fig 5b). This is now clarified in the Figure 5 caption text.

Figure 5:

T_{max} values of the sum thermograms are shown with dashed lines. In panel b) Tmax values of only Scots pine experiment 1 and Scots pine experiment 4 are shown for clarity.

Line 343. "Some signatures of thermal decomposition are visible as well, but overall this appears to play a minor role, with very small effects on Tmax in most individual ion cases". Please explain what you mean by signatures of thermal decomposition. Do you mean multiple peaks in the thermogram? Please explain how you are treating multiple peaks in thermograms e.g. disregarding or deconvolving multipeak thermograms. Can you be more specific than 'small effects'?

By "signatures of thermal decomposition" we indeed meant either multiple peaks or pronounced tailing in thermogram of a single fitted composition. This kind of behaviour was only observed in a handful of signals while the total amount of fitted peaks totals more than 600 compounds. Therefore, Tmax of these multiply peaking thermograms is assigned to the highest peak, which is usually the first mode of the signal and the second mode is disregarded. The second mode could be deconvoluted from the first mode in clear multiple-peak cases, but more often than not such deconvolution, e.g. by fitting multiple peaks, appeared not feasible. The main reason for that is that the applicable peak *shapes* generally remain ambiguous (Lopez-Hilfiker et al., ACP, 2015; Stark et al., EST, 2017; Schobesberger et al., ACP, 2018; Buchholz et al., ACPD, 2019). Therefore, we decided not to involve such deconvolution in this analysis but note that by neglecting secondary thermogram "modes", the use of Tmax values tends to somewhat underestimate volatility (e.g. as expressed by derived saturation vapour concentrations).

The sentence "very small effects on Tmax in most individual ion cases" is poor choice of wording and should read "very small effects on the thermogram in most individual cases" as tailing of additional peaks in the thermogram would hardly affect the allocation of the Tmax value, irrespective of possibly first deconvoluting the thermogram. This is now corrected to the text at line 371.

Line 344. “Consequently, the shifts to higher desorption temperatures as observed in the sum thermograms (Fig.5) are essentially seen throughout each respective spectrum of individual unit mass thermograms, although the contribution of thermal decomposition appears to increase concurrently.” I am unsure what this means. It sounds like at all unit masses, you are seeing increasing Tmax as you increase the experiment number.

The sentence clearly needs clarification. It has been rephrased as:

Line 373:
The resistance to thermal desorption at each unit mass appears to increase with increasing strength of oxidation in the α-pinene experiments, as is observed in the sum thermograms (Fig. 5), while the contribution of thermal decomposition appears to increase concurrently. The Scots pine experiments show similar effects between Scots pine experiments 1-4, but the change is not as pronounced as with α-pinene experiments and cannot be as clearly attributed to a single factor such as oxidative strength.

Line 369. “...manifests in the disappearance of SVOC...“. Disappearance or reduction?

“Reduction” is the more appropriate term. Term changed in the text at line 404.

Line 397. Just OH exposure or oxidation in general if ozonolysis is included?

The text is rephrased to “oxidative strength” at line 436.

Technical Corrections

Line 44. Missing word. “The volatility of a specific compounds in turn is determined by both its molar mass and functional group composition”

Fixed the sentence.

Line 300. There is no Sect. 3.4.

Corrected the section numbering.

Line 432. Some missing words.

Corrected the text to past sentence.

Canagaratna, M. R., Jimenez, J. L., Kroll, J. H., Chen, Q., Kessler, S. H., Massoli, P., Hildebrandt Ruiz, L., Fortner, E., Williams, L. R., Wilson, K. R., Surratt, J. D., Donahue, N. M., Jayne, J. T. and Worsnop, D. R.: Elemental ratio measurements of organic compounds using aerosol mass spectrometry : characterization , improved calibration , and implications, Atmos. Chem. Phys., 15, 253–272, doi:10.5194/acp-15-253-2015, 2015.

Decarlo, P. F., Kimmel, J. R., Trimborn, A., Northway, M. J., Jayne, J. T., Aiken, A. C., Gonin, M., Fuhrer, K., Horvath, T., Docherty, K. S., Worsnop, D. R. and Jimenez, J. L.: Aerosol Mass Spectrometer, , 78(24), 8281–8289, doi:10.1021/ac061249n, 2006.

Faiola, C. L., Buchholz, A., Kari, E., Yli-Pirilä, P., Holopainen, J. K., Kivimäenpää, M., Miettinen, P., Worsnop, D. R., Lehtinen, K. E. J., Guenther, A. B. and Virtanen, A.: Terpene Composition Complexity Controls Secondary Organic Aerosol Yields from Scots Pine Volatile Emissions, Sci. Rep., 8(1), 1–13, doi:10.1038/s41598-018-21045-1, 2018.

Faiola, C. L., Pullinen, I., Buchholz, A., Khalaj, F., Ylisirnio, A., Kari, E., Schobesberger, S., Yli-juuti, T., Miettinen, P., Holopainen, J. K. and Kivima, M.: Secondary Organic Aerosol Formation from Healthy and Aphid- Stressed Scots Pine Emissions, , doi:10.1021/acsearthspacechem.9b00118, 2019.

Hakola, H., Tarvainen, V., Bäck, J., Ranta, H., Bonn, B., Rinne, J. and Kulmala, M.: Seasonal variation of mono- and sesquiterpene emission rates of Scots pine, Biogeosciences, 3, 93–101, 2006.

Kourtchev, I., Fuller, S. J., Giorio, C., Healy, R. M., Wilson, E., Connor, I. O., Wenger, J. C., Mcleod, M., Aalto, J., Ruuskanen, T. M., Maenhaut, W., Jones, R., Venables, D. S., Sodeau, J. R., Kulmala, M. and Kalberer, M.: Molecular composition of biogenic secondary organic aerosols using ultrahigh-resolution mass spectrometry : comparing laboratory and field studies, Atmos. Chem. Phys., 14, 2155–2167, doi:10.5194/acp-14-2155-2014, 2014.

Mohr, C., Thornton, J. A., Heitto, A., Lopez-hil, F. D., Lutz, A., Riipinen, I., Hong, J., Donahue, N. M., Hallquist, M., Petäjä, T., Kulmala, M. and Yli-juuti, T.: Molecular identification of organic vapors driving atmospheric nanoparticle growth, Nat. Commun., 10(4442), 1–7, doi:10.1038/s41467-019-12473-2, 2019.

Palm, B. B., Campuzano-jost, P., Ortega, A. M., Day, D. A., Kaser, L., Jud, W., Karl, T., Hansel, A., Hunter,

J. F., Cross, E. S., Kroll, J. H., Peng, Z., Brune, W. H. and Jimenez, J. L.: In situ secondary organic aerosol formation from ambient pine forest air using an oxidation flow reactor, , 2943–2970, doi:10.5194/acp-16-2943-2016, 2016.

Composition and volatility of SOA formed from oxidation of real tree emissions compared to ~~single~~ simplified VOC-systems

Arttu Ylisirniö[1], Angela Buchholz[1], Claudia Mohr[2,3], Zijun Li[1], Luis Barreira[1,4], Andrew Lambe[5], Celia Faiola[1,6], Eetu Kari[1,a], Taina Yli-Juuti[1], Sergey A. Nizkorodov[7], Douglas R. Worsnop[5], Annele Virtanen[1], and Siegfried Schobesberger[1]

[1]Department of Applied Physics, University of Eastern Finland, Kuopio, Finland
[2]Institute of Meteorology and Climate Research, Karlsruhe Institute of Technology, Karlsruhe, Germany
[3]Department of Environmental Science and Analytical Chemistry, Stockholm University, Stockholm, Sweden
[4]Atmospheric Composition Research, Finnish Meteorological Institute, Helsinki, Finland
[5]Center for Aerosol and Cloud Chemistry, Aerodyne Research, Inc., Billerica, MA, USA
[6]Department of Ecology and Evolutionary Biology, University of California, Irvine, Irvine, USA
[7]Department of Chemistry, University of California, Irvine, Irvine, USA
[a]currently at: Neste Oyj, Espoo, Finland

Correspondence to: Arttu Ylisirniö (arttu.ylisirnio@uef.fi)

Abstract.

Secondary organic aerosol (SOA) is an important constituent of the atmosphere where SOA particles are formed chiefly by the condensation or reactive uptake of oxidation products of volatile organic compounds (VOC). The mass yield in SOA particle formation, as well as the chemical composition and volatility of the particles are determined by the identity of the VOC precursor(s) and the oxidation conditions they experience. In this study, we used an oxidation flow reactor to generate biogenic SOA from the oxidation of Scots pine emissions. Mass yields, chemical composition, and volatility of the SOA particles were characterized and compared with SOA particles formed from oxidation of α-pinene and of a mixture of acyclic/monocyclic sesquiterpenes (farnesenes and bisabolenes), which are significant components of the Scots pine emissions. SOA mass yields for Scots pine emissions dominated by farnesenes were lower than for α-pinene, but higher than for the artificial mixture of farnesenes and bisabolenes. The reduction in the SOA yield in the farnesenes and bisabolenes dominated mixtures is due to exocyclic C=C bond scission in these acyclic/monocyclic sesquiterpenes during ozonolysis leading to smaller and generally more volatile products. SOA particles from the oxidation of Scots pine emission had similar or lower volatility than SOA particles formed from either of single precursor or a simple mixture of VOCs. Applying physical stress to the Scots pine plants increased their monoterpene emissions, especially monocyclic β-phellandrene, which further decreased SOA particle volatility and increased SOA mass yield. Our results highlight the need to account for the chemical complexity and structure of real-world biogenic VOC emissions and stress-induced changes to plant emissions when modelling SOA production and properties in the atmosphere. These results emphasize that simple increase or decrease of relative monoterpene and sesquiterpene emissions should not be used as indicator of SOA particle volatility.

1 Introduction

Secondary organic aerosol (SOA) formed from oxidation of volatile organic compounds (VOCs) contributes a large fraction to the total aerosol mass in the boreal forests of the northern hemisphere (Hallquist et al., 2009; Jimenez et al., 2009; Riipinen et al., 2012). The chemical transformation of primary VOC emissions to SOA particles, which have an important climate impact (Hallquist et al., 2009), is a complicated cascade of gas-phase oxidation and multi-phase aging reactions. The physical properties of SOA are dictated by the chemical complexity of the initial VOC emissions and the oxidative conditions they experience (Glasius and Goldstein, 2016).

The formation and growth of SOA particles is often described by the absorptive partitioning of organic vapours (e.g. terpenoid oxidation products) between gas and particle phase (Donahue et al., 2011; Pankow, 1994). The main property determining how readily organic molecules enter and stay in the particle phase is their volatility, usually expressed as saturation vapor pressure (*Psat*) or saturation mass concentration (C^*) in air. The volatility of a specific compound is~~s~~ in turn determined by both its molar mass and functional group composition (Capouet and Müller, 2006; Pankow and Asher, 2008). Oxidation of a single VOC precursor produces a wide variety of semi- and low-volatility compounds, which are able to condense into the particle phase according to their C^*. The uptake of oxidation products may also involve or be facilitated by heterogeneous reactions.

In boreal forest environments, VOC emissions are dominated by monoterpenes. As the globally most important monoterpene (Spanke et al., 2001), α-pinene has hence been most commonly used as a model species in laboratory SOA studies. Consequently, α~~a~~-pinene has been used as a proxy for all other monoterpenes in atmospheric models using its properties to describe the atmospheric oxidation and contribution to SOA particles of all other monoterpenes (Holopainen et al., 2017; Yassaa et al., 2012).

However, the VOC emission patterns of vegetation vary significantly depending on locations, environmental conditions and even genotypes of each plant. Moreover, differences in emissions can be even found between two plants of the same species with same age located in the same environment (Bäck et al., 2012; Hakola et al., 2017; Holopainen and Gershenzon, 2010). Even though the VOC emissions from boreal forests are thought to mostly consist of monoterpenes, Hellén et al., (2018) recently showed a significant contribution of sesquiterpenes to the total VOC budget in boreal forests. This finding is in line with an earlier study by Hakola et al. (2017) that showed high emissions of sesquiterpenes measured from branch enclosures in a coniferous forest in Finland during early spring and late autumn. Mixtures of different VOCs as well as different trace gases like NOx, CO and sulfuric acid also influence the oxidant reactivity and oxidant product distribution compared to single VOC precursor oxidation (McFiggans et al., 2019; Ng et al., 2017). These results highlight~~s~~ the need to use real emissions as precursors while exploring the physical and chemical properties of SOA particles.

In this study, we present results from a state-of-the-art suite of instruments used to investigate the VOC emission profile of Scots pine saplings (Pinus sylvestris) and subsequent SOA formation from these VOCs in an oxidation flow reactor (OFR). The central instrument in this work is a Filter Inlet for Gases and AEROsols, coupled to a high-resolution time-of-flight Chemical Ionization Mass Spectrometer (FIGAERO-CIMS; Aerodyne Inc. and Tofwerk AG; Lopez-Hilfiker et al., 2014), which allowed us to characterize the composition and thermal desorption behavior of the SOA particles. For comparison, we performed the same measurements for SOA formed from α-pinene in the same OFR. Prompted by a strong contribution of farnesenes to the emissions from our plants, we also examined SOA formation from a mixture of acyclic/monocyclic sesquiterpenes with major contribution from isomeric farnesenes and bisabolenes. This is the first volatility measurement of SOA particles formed from the oxidation of farnesene and bisabolene since earlier studies involving these sesquiterpenes have focused on the gas-phase chemistry (Kim et al., 2011; Kourtchev et al., 2009, 2012) or the chemical composition of the SOA particles (Jaoui et al., 2017). Our results show surprising impacts of the VOC mixture on the SOA particle volatility compared to SOA particles formed from a single VOC compound.

2 Materials and methods

2.1. VOC measurements and SOA production

We conducted experiments with SOA generated from the ozonolysis and photo-oxidation of VOCs by hydroxyl radicals (OH) in a Potential Aerosol Mass (PAM) OFR (Kang et al., 2007; Lambe et al., 2011) in the absence of seed particles. The experimental setup is similar to that in our previous study (Buchholz et al., 2019). A schematic of the setup is shown in Figure 1 and all experimental conditions are listed in Table 1 and Table 2. We provide a very brief description of the experimental setup here and more detailed information can be found in the supplement material (Sect. S2). A flow containing 200 to 400 ppb of the investigated VOCs was mixed with an O_3 containing flow directly before entering the OFR. With two UV lamps (254 nm), O_3 was photolyzed to $O(^1D)$ which reacted with water vapor to produce OH radicals. A wide range of OH exposure was achieved by adjusting the voltage of 254-nm UV lamps in the OFR and changing the O_3 concentration. Overall, the integrated OH exposure in the OFR ranged from approx. 6.6×10^{10} to 2.5×10^{12} molec cm^{-3} s across all experiments as calculated according to methods described by Peng et al. (2015, 2016). This range of OH exposure corresponds to 0.5 to 19 equivalent days of atmospheric aging at an OH concentration of 1.5×10^{6} molec cm^{-3} (Palm et al., 2016). In all experiments, the operation temperature of the OFR was 25 or 27 ˚C and relative humidity (RH%) was between 40 % to 60 %. For the Scots pine experiments, VOCs were introduced by flushing purified air through a plant enclosure (Tedlar®) containing a 6-year-old Scots pine sapling. In the α-pinene (Sigma Aldrich, 98 % purity) and sesquiterpene mix (mixture of acyclic/monocyclic sesquiterpenes, Sigma Aldrich) experiments the VOCs were introduced into a flow of clean nitrogen by using a diffusion source or a dynamic dilution system (Kari et al., 2018). For the Scots pine experiment 4, the

plant was injured by making four 0.5 - 1 cm^2 cuts into the bark of the plant exposing resign pools and thus, increasing the VOC emissions.

The VOC mixing ratios entering the OFR were continuously monitored using a proton-transfer-reaction time-of-flight mass spectrometer (PTR-MS, PTR-TOF 8000, Ionicon Analytik Inc.) directly upstream of the OFR inlet but before the addition of O_3 to the system. All reported mixing ratios were corrected for this dilution and represent the conditions at the inlet of the OFR. In addition, to resolve the mixture of terpenoid emissions emitted by the Scots pine sapling, we collected two cartridge samples (Tenax-TA, MARKES etc.) at the beginning of the Scots pine experiment 1 and at the end of the Scots pine experiment 4 for off-line analysis using a Thermal Desorption Gas Chromatograph Mass Spectrometer (TD-GC–MS, TD: Perkin Elmer, ATD 400, USA, GC–MS: Hewlett Packard, GC 6890, MSD 5973, USA). PTR-MS calibration procedure is described in Sect. S3.

The measured emission profiles from the Scots pine showed a strong contribution of α- and β-farnesene (Fig. 2), which are acyclic sesquiterpenes. Therefore, we conducted follow up experiments under similar oxidative conditions using a commercially available mixture of acyclic/monocyclic sesquiterpenes to investigate the effect of such biogenic, unsaturated, acyclic/monocyclic VOCs on SOA properties. This sesquiterpene mixture consisted of isomers of farnesenes and bisabolene, both of which are found in the emissions of coniferous trees as well as the emissions of Scots pines in this study (Blande et al., 2009; Holopainen and Gershenzon, 2010). For a detailed description of the mixture see Table S1 and Fig. S1. For those follow-up experiments, a nominally identical OFR was used ("PAM 2"). However, to recreate the same OH exposure and particle composition (as characterised by particle oxidation ratio, see below) a different combination of light intensity, residence time, and O_3 concentration was necessary in the follow-up experiments. Thus, the results are presented separately and marked PAM1 or PAM2.

2.2. SOA particles characterization

SOA particles were examined with a suite of instruments sampling from the outlet of the OFR: a High-Resolution Time-of-Flight Aerosol Mass Spectrometer (AMS, Aerodyne Research Inc.), a Scanning Mobility Particle Sizer (SMPS, TSI Inc., Model 3082 with TSI Model 3775 Condensation Particle Counter) and a FIGAERO-CIMS using the iodide ionization scheme (Lee et al., 2014). AMS and SMPS were used to continuously monitor the output SOA particle mass and size distribution from the OFR to determine the point when the particle concentrations and distributions had stabilized for a given OFR condition. Then the filter collection for FIGAERO-CIMS was started, so that only steady-state SOA was sampled. More information about these other instruments is given in Sect. S4.

The FIGAERO-CIMS was used to characterize the volatility and chemical composition of the SOA particles for those

organic compounds sensitive to iodide cluster ionization. Briefly, in the ionization region of the instrument, operated at 100 mbar pressure, an I^- anion preferably clusters with a neutral molecule M which contains hydroxy-, hydroperoxy-, carboxyl- or peroxycarboxyl-groups ~~oxygen or OH group~~ in their structure. The neutral molecule is then observed as $[M+I]^-$ in the mass spectrometer (Iyer et al., 2017; Lee et al., 2014). In the presence of water, collision of an $[H_2O+I]^-$ anion cluster with M may produce the same result. In some cases, the $[M+I]^-$ cluster breaks apart leading to deprotonation of the neutral molecule, which is then observed as $[M-H]^-$, and possibly to other ion fragments. This phenomenon has also been observed in earlier studies (e.g. Lee et al., 2014). For the further analysis, we assume that deprotonation is the only mechanism of declustering, as it is one known to potentially follow already from relatively soft collisions. Additional declustering may happen by more energetic collisions in the lower-pressure regions of the mass spectrometer (Passananti et al., 2019).

In the FIGAERO inlet, the aerosol particles were sampled through 2 m stainless steel tubing (outer diameter 6 mm) onto a Teflon filter (Zefluor 2 µm PTFE Membrane filter, Pall Corp.) for 2-5 min with a collection flow of 2 L min^{-1}. The particles were then evaporated into the instrument with gradually heated nitrogen flow with a heating rate of 11.6 (K/min) up to 200 ˚C over a period of 20 min and then kept at 200˚C for additional 10 min to evaporate any residual compounds. This results in temperature-dependent ion signals for each observed mass spectrum peak (thermograms) that can be related to the volatility of the collected organic compounds (Lopez-Hilfiker et al 2014, and Lopez-Hilfiker et al., 2015). In this study, two slightly different FIGAERO inlets were used: one in conjunction with the initial experiments using the "PAM 1" reactor ("FIGAERO 1"), the other when using the "PAM 2" reactor later-on ("FIGAERO 2"). The CIMS themselves were nominally identical, and both of the FIGAERO inlets followed the identical principles and were operated identically. The differences were in the detailed design of the FIGAERO inlets, e.g., the shape of filter collection tray and exact positioning of temperature sensor. These changes lead to apparent shifts of the measured thermograms. To account for this, we performed instrument specific calibrations for both FIGAERO inlets, which is described in more detail in Sect. 2.2.2.

A blank measurement, meaning a measurement with no particles collected on the filter, was performed before each measurement to make sure the filter was clean of residual compounds and to determine any instrument artefacts. The assure that filter did not contain any particles, collection flow leading to the filter was shut down between actual measurements. These blank measurements were also considered in the data-analysis. The relatively high collected particle mass loading (between 500 and 1350 ng) on the filter ensured that the majority of the signal came from the evaporating SOA particles, and that the instrument background/artefacts were neglectable. The FIGAERO filter was also visually inspected daily and replaced when needed.

2.2.1 FIGAERO-CIMS data-analysis

The FIGAERO-CIMS data was analysed with the MATLAB-based tofTools (Junninen et al., 2010) software, including the identification of elemental compositions (creation of peak lists) based on the high resolution (HR) peak fitting with mass accuracy of 5 ppm. All data shown here is based on the HR-fitting of the mass spectra using peak lists covering the full spectra. The presented mass values are those of the neutral composition (*M*), derived by subtracting the molecular mass of I^- when $[M+I]^-$ was observed or by adding the molecular mass of *H* when $[M-H]^-$ was observed. The assigned formulas were constrained to contain only C, H and O elements; any signal peak appearing to contain other elements was considered background and excluded from further analysis. This background consisted mostly of fluorine containing compounds, which we assume to originate from the FIGAERO inlet manifold or the collection filter, both of which are made of PTFE.

2.2.2 T_{max} to saturation concentration calculations

Typically, the thermograms collected from the heat-induced SOA evaporation in the FIGAERO filter comprise a clearly defined peak, i.e., a temperature at which the largest signal is observed (T_{max}). It has been shown that T_{max} correlates with the volatility of the desorbing organic compound, typically expressed as saturation concentration C^*, at least for systems with limited number of compounds (Bannan et al., 2018; Lopez-Hilfiker et al., 2014). We determined the relationship between T_{max} and C^* for both FIGAERO inlets independently, based on the results of calibration experiments using a series of polyethylene glycols (PEG) with known saturation pressures P_{sat} (Pa) at reference temperature of 298.15 K (Bannan et al., 2018; Krieger et al., 2018). All reported C^* and P_{sat} values are thus contrasted to this temperature. The calibration method and resulting parameters are described in the supplementary material Sect ~~S3~~S5.

2.2.3 SOA yield calculations and theoretical yields

From the amount of consumed precursor VOC (ΔVOC), and the condensed (i.e., particulate) organic mass (ΔC_{OA}) one can calculate the effective SOA mass yield *Y* by

$$Y = \frac{\Delta C_{OA}}{\Delta VOC_{MT+SQT}}. \quad (1)$$

The subscripts here refer to monoterpenes (MT) and sesquiterpenes (SQT), which were the dominant contributors~~ion~~ to SOA formation in these experiments. The ΔVOC_{MT+SQT} (µg m^{-3}) was calculated from the difference of the total concentrations of monoterpenes and sesquiterpenes entering the OFR and the VOC concentration exiting the OFR, which ~~is~~ was quantified by the PTR-MS. Measured mixing ratios of both MTs and SQTs exiting the OFR were <1 ppb. The condensed organic mass ΔC_{OA} (µg m^{-3}) was monitored using the SMPS number size distribution and assuming a particle density of 1.3 g cm^{-3} for all measurements (Faiola et al., 2018). No wall-loss correction was applied to the VOC and particle measurements. ~~However, the same length of tubing was used for all the measurements so possible wall losses are assumed to be nearly~~

~~identical.~~However, because the VOC measurement was made almost immediately before the inlet of the OFR and formed SOA size distribution was roughly identical between different experiments, we assume that possible sampling line wall losses have minor impact on our SOA yield calculations.

The SOA yield can also be expressed using the approach of Odum et al. (1996), which allows for formally breaking down SOA formation into the contribution of several VOC species:

$$Y = \Delta C_{OA} \sum_i \frac{\alpha_i K_i}{1+K_i \Delta C_{OA}}, \quad (2)$$

where α_i is a proportionality constant relating the amount of reacted VOC (precursor) to the total concentration of species *i* (oxidation product) and K_i is the partitioning coefficient for species *i*. We use a two-product version of equation (2), which is common in modeling applications.

2.3 Scots pine sapling treatment

Due to scheduling constraints, the experiments were conducted in early autumn outside of the most active emission time for scots pines. To circumvent this, Scots pine saplings (6 years old) were stored in a cold room throughout the summer to maintain winter dormancy. They were removed from the cold room ~1 month before experiments to initiate spring phenology and metabolism – the time of year when Scots pines are active with new shoot growth. At least 24 hours before the SOA experiments, saplings were transported to the laboratory and a dynamic Teflon plant enclosure was installed around the plant foliage. The Teflon enclosure (custom-built; Jensen Inert Products, Inc.) was secured to the plant stem with two cable ties. The plant enclosure was flushed with 5 L min^{-1} purified compressed air and operated under positive pressure to push enclosure air into the flow reactor through PFA tubing. The flow of plant enclosure air into the OFR was regularly measured in-line and maintained at 1.7-1.9 L min^{-1}. Three LED lamps were placed around the plant to provide photosynthetically active radiation (PAR) similar to ambient levels in Finland.

3. Results and discussion

3.1 Scots pine emission patterns

The VOC emissions from the Scots pine sapling were mainly composed of monoterpenes and sesquiterpenes. The emissions were monitored on-line with PTR-MS and off-line with TD-GC-MS, the latter allowing us to better speciate the VOCs by distinguishing between isomers. In Fig. 2 we show the chemical structures of the most abundant compounds (see Table S2

for full list), along with the relative concentrations of the individual monoterpenes and sesquiterpenes, as measured by TD-GC-MS.

Among the monoterpenes, β-phellandrene had the highest concentration, followed by 3-carene, d-limonene, β- and α-pinene, in this order. These five monoterpenes accounted for 90 % of all monoterpenes in all experiments. Among the sesquiterpenes, β- and α-farnesene, and α-bisabolene were the most abundant species, accounting for about 95 % of all sesquiterpenes. All sesquiterpenes combined accounted for 55 % - 70 % of the total VOC mass concentration in the Scots pine experiments 1-3, and for 40 % in the Scots pine experiment 4, based on PTR-MS measurements. Relating these results to the ambient pine emission characterizations by Bäck et al. (2012), our Scots pine sapling may be classified as a "3-carene" chemotype, due to the higher emission of 3-carene. The fraction of sesquiterpene emissions in our study was considerably higher than expected from the ambient pine emission measurements of SQT/MT ratio of typically ~ 0.1 by mixing ratio (Hellén et al., 2018). The used scots pine sapling was infested with herbivores creating biotic stress for the plant changing the VOC emission pattern. This type of biotic stress is natural, especially in a changing climate where insect outbreaks are predicted to become more frequent (Bale et al., 2002; Jactel et al., 2019).

During the Scots pine experiments 1-3, the VOC levels were slowly decreasing over time. Therefore, after the end of the Scots pine experiment 3, we made four 0.5-1 cm^2 cuts to the Scots pine sapling's stem, with the goal of increasing VOC emissions to continue the production of sufficient SOA. The wounds exposed plants resin pools in the stem and increased the measured monoterpene concentrations compared to pre-cutting concentrations by roughly doubling them. Sesquiterpene concentrations, however, were not significantly affected. The compound that increased most was β-phellandrene, emissions of which had also been shown to increase with bark beetle infestation damage (Amin et al., 2012; Faiola et al., 2018). Such damage essentially consists of cuts into the stem as the bark beetle feeds on the plant, hence that observation is consistent with expectations.

3.2 SOA mass yields

In Figure 3, we plot SOA yields against condensed organic mass C_{OA} from each experiment, split into two panels, according to which of the two PAM reactors was used (Fig. 3a, "PAM 1"; Fig. 3b, "PAM 2"). Note that a similar organic mass range was covered in all experiments.

The Scots pine experiments 1-3 featured sesquiterpene-to-monoterpene ratios (SQT/MT) by mass ratio between 1.2 and 2 (color-coding in Fig. 3a). The SOA yields obtained during these experiments are consistent with each other in a sense that all the data points are well described by the same two-product model (orange line). The SOA yields resulting from Scots pine experiment 4 are about 30% larger, even though SQT/MT was substantially smaller than in experiments 1-3. Earlier study by

(Faiola et al., 2018) reported a positive correlation with SOA yield and SQT/MT ratio of VOC's measured from Scots pine seedlings in a flow tube experiment similar to our study.

To understand the unexpected suppression of SOA yield at higher relative SQT concentrations, we also measured SOA yields for a synthetic sesquiterpene mixture containing isomers of farnesene and bisabolene. A different PAM reactor had to be used, therefore we compare those results to a reference α-pinene experiment using the same reactor (Fig. 3b). The ingoing VOC concentration was varied for both precursors and yield measurements were conducted in order to cover the C_{OA} range of the Scots pine experiments. A single FIGAERO measurement was made for both precursors and the corresponding sampling conditions are marked with circles in Fig. 3b. The comparison shows a clearly lower yield for the sesquiterpene mixture than for α-pinene, which is in line with results shown in Fig. 3a. Note that the medium and low exposure a-pinene measurements in PAM 1 show similar yield values as those in the reference experiment in PAM 2, but the yield of the high exposure experiment is significantly lower. This is consistent with the extensive fragmentation expected inside the PAM reactor under strong oxidative conditions which reduces the effective SOA yield (Lambe et al., 2012).

We conclude that the increase in SOA yield in the Scots pine experiment 4, compared to the Scots pine experiments 1-3, is likely due to the large relative increase in emitted monoterpenes, especially ~~.~~ β-phellandrene, caused by cutting the sapling (Fig. 2). We surmise that β-phellandrene must have a high SOA yield, possibly comparable to that of d-limonene, which has been reported in a range of 50-60 % (Berg et al., 2013; Lee et al., 2006; Surratt et al., 2008), and which shares some structural similarity with β-phellandrene (Fig. 2). Mackenzie-Rae et al. (2017) measured SOA yields of α-phellandrene, an isomer of β-phellandrene with an endocyclic C=C bond and found the SOA yield to be around twice that of α-pinene, reaching up to 100 %. While those yield numbers are not directly comparable to our results, they qualitatively indicate that SOA yields from monocyclic monoterpenes, with endocyclic C=C bonds, could be higher than those from the more commonly studied bicyclic monoterpenes, such as α-pinene.

It is instructive to compare our SOA yield results to results of earlier experiments that used (stressed) Scots pines. Faiola et al. (2018) studied SOA formation from emissions of herbivore-stressed Scots pines in a custom-made OFR where the main SQT was β-caryophyllene. There the increasing SOA yields with increasing SQT contribution to the precursor mix was explained by the much higher SOA yield of β-caryophyllene (Faiola et al., 2018). In chamber studies with emissions of aphid stressed Scots in which farnesenes were the dominant SQT species, SOA yields decreased with increasing SQT contribution for ozonolysis reaction while no change was observed for pure OH reaction experiments (Faiola et al., 2019). In our experiments in the PAM reactor, the ratio between O_3 and OH exposure was in the range of 10^5 which is comparable to ambient levels (Kang et al., 2007). Due to the very fast reaction with O_3, more than 80 % of any SQT is expected to react with O_3 under these conditions (calculated with methods described by Peng et al. (2015, 2016)). Thus, the SOA yield should decrease with increasing amounts of farnesene as described for the ozonolysis reaction pathway in Faiola et al. (2019).

The reason for this different behavior of the two SQT types is based on their molecular structure. β-caryophyllene is a bicyclic compound with one endo- and one exo-cyclic C=C bond whereas farnesene isomers are acyclic compounds with 4 C=C bonds. In the (photo-)oxidation process, both ozone and OH-radicals break the C=C bonds and thus the carbon back bone of farnesene into small fragments. Already a single oxidation step creates decreases the number of carbons from 15 to 5 - 12 (Kourtchev et al., 2009, 2012). In case of the bicyclic β-caryophyllene, such fragmentation is expected to be much less prominent (Jaoui et al., 2003, 2013).

There may be further interactions between the small, most likely volatile farnesene reaction products and the other oxidation products suppressing the particle formation further as recently described by (~~Mcfiggans~~ McFiggans et al., 2019).

3.3 SOA composition

Figure 4 shows mass spectra integrated over the heating period of FIGAERO-CIMS measurements normalized to the maximum signal and molecular mass adjusted to neutral compositions (Sect. 2.2.1). The results are grouped in two portions as two different PAM reactors and FIGAERO inlets were used in the measurements (Sect. 2.2). The α-pinene measurements (Fig. 4, top row) show a decrease in the average molecular weight with increasing OH exposure, which is consistent with the decrease in SOA mass yields as a function of OH exposure observed in Fig. 3 and also observed in an earlier study (Hall et al., 2013).

The distribution of molecular weights of compounds in the sesquiterpene mixture SOA particles (Fig. 4, right) shifted more towards smaller molecular masses than in any other experiment. We explain this by the acyclic molecular structure of the sesquiterpene compounds leading to their more efficient splitting into smaller products (fragmentation) during oxidation (see Sect. 3.2). The α-pinene reference spectra differ slightly from other α-pinene measurements, even though OH-exposure falls between medium and high exposure (Table 2).

The difference might be due to the different residence time inside the PAM reactor (120 vs 160 s) or from the higher mixing ratio of VOCs in the experiment done with the PAM2 reactor. The FIGAERO mass spectra distribution of SOA formed from the Scots pine emissions had most similarities to high-exposure α-pinene SOA, with almost all compounds appearing within a single mode, roughly cent~~e~~red on the monomer mode of the other α-pinene experiments.

Table 3 shows the average carbon oxidation states (OSc) (Kroll et al., 2011) and the average O:C ratio, calculated from both AMS and FIGAERO data. The average chemical composition is also calculated from FIGAERO data. All FIGAERO data values are weighted averages, using the integrated signal strength of each ion thermogram as weights. The range of values

calculated from the FIGAERO data represents the spread of different compounds in the mass spectrum, which we will investigate below.

In the α-pinene experiments with PAM1, the average O:C and OSc increases with the increasing oxidative strength as expected while the average carbon chain length decreases. In terms of the average O:C or OSc, the Scots pine experiments most closely correspond to the medium exposure α-pinene experiment. Interestingly, all Scots pine experiments appear broadly similar from this viewpoint, even though experiment 4 is associated with emissions dominated by monoterpenes (i.e., much smaller SQT/MT) and clearly higher SOA yields (Figs. 2 and 3a). However, the Scots pine SOA particles differ from each other and from other experiments in other ways, as we will see in Sect. 3.4.

3.~~2~~ 4 SOA volatility

In Figure 5, we show normalized "sum" thermograms, calculated by summing up the thermograms from all ions that contain only C, H and O atoms. With these sum thermograms, the average thermal desorption behaviour can be compared across multiple experiments. While viewing the thermograms, it is important to know that the thermal decomposition during the aerosol desorption from the FIGAERO filter often manifests as signal at relatively high desorption temperatures, which may appear as shoulders to the main peak, but it can appear as simple peaks as well (e.g., Lopez-Hilfiker et al., 2015; Schobesberger et al., 2018).

For the α-pinene experiments, the sum thermograms reveal a clear increase of T_{max} (dashed vertical lines in Fig. 5a) with increasing oxidative exposure. As we have shown above, this change is concurrent with a decrease in molecular size and an increase in average O:C-ratio (Fig. 4 and Table 3). Together, these observations imply that α-pinene photo-oxidation successively forms compounds with lower volatility. Evidently, the oxidation reactions are both fragmenting, which generally increases volatility, as well as functionalizing, which generally decreases volatility (Capouet and Müller, 2006; Pankow and Asher, 2008). The clearly increasing T_{max} values observed with FIGAERO suggests a net decrease in volatility due to these processes overall, for the condensed-phase constituents, consistent with the results of isothermal evaporation experiments performed using the same (but size-selected) aerosol (Buchholz et al., 2019).

The sum thermograms for the Scots pine experiments gradually shift towards yet higher desorption temperatures (Fig. 5b); all their T_{max} values are higher than those of any of the α-pinene experiments (Fig. 5a). In particular, SOA particles from Scots pine experiment 4 are the most resistant to thermal desorption. That experiment was also the only one with plant emissions clearly dominated by monoterpenes (Fig. 2), specifically with β-phellandrene being the most abundant, which we associated above with relatively high observed SOA yields (Sect. 3.1). That specific VOC mix in the Scots pine experiment 4 is unique within our study here. It is plausible that this mix is also directly responsible for producing SOA with the lowest

effective C^* as suggested by the results of our FIGAERO measurements (Fig. 5, as well as our more detailed discussion below).

We suggest that the increased desorption temperatures for the Scots pine experiments 1-3 relative to the α-pinene experiments is due to the large contribution of acyclic sesquiterpenes (in particular farnesenes, Fig. 2) to the plant emissions in those experiments. We tested this hypothesis via our follow-up experiments using the PAM 2 reactor and FIGAERO 2 (Fig. 5c). These experiments yielded sum thermograms for SOA particles formed from the farnesene-dominated sesquiterpene mixture, and those from α-pinene using the same setup, for reference. The reference α-pinene SOA particles had a $\langle O:C \rangle_{AMS}$ of 0.77, similar to those in the medium and high exposure α-pinene case. Indeed, the sum thermogram T_{max} value for the sesquiterpene mix case is about 10 °C higher than for the reference α-pinene case, confirming that the strong contribution of farnesene and sesquiterpenes with similar structures leads to the effectively lower-volatility aerosol particles (as measured by FIGAERO) in the Scots pine experiments 1-3 compared to α-pinene SOA particles. As mentioned earlier (Sect. 2.2), a quantitative comparison of thermograms between Fig. 5c and Figs. 5a-b, including comparison of T_{max} values, is not straightforward, due to the differences in the respective experimental setups. However, we will deal with this issue below.

We provide a more extended discussion of our examination of SOA volatilities, which includes graphical depictions of the individual ion thermograms, in the supplement material (Sect. ~~S4~~S6). When looking at individual experiments, the T_{max} value for each ion broadly depends on the molecular weight of the ion, as expected. However this dependency seems to differ in scale between experiments. Some signatures of thermal decomposition are visible as well, but overall this appears to play a minor role, with very small effects on ~~T_{max}~~ the thermogram ~~-~~in most individual ion cases.

The resistance to thermal desorption at each unit mass appears to increase with increasing strength of oxidation in the α-pinene experiments, as is observed in the sum thermograms (Fig. 5), while the contribution of thermal decomposition appears to increase concurrently. The Scots pine experiments show similar effects between Scots pine experiments 1-4, but the change is not as pronounced as with α-pinene experiments and cannot be as clearly attributed to a single factor such as oxidative strength.

~~Consequently, the shifts to higher desorption temperatures as observed in the sum thermograms (Fig. 5) are essentially seen throughout each respective spectrum of individual unit mass thermograms, although the contribution of thermal decomposition appears to increase concurrently.~~

Previous studies have indicated that the T_{max} value of individual thermograms largely remains controlled by the C^* of the respective compound, even when a substantial fraction of the signal is the result of thermal decomposition of different, larger structures (e.g. Schobesberger et al., 2018). The reason is that this decomposition typically occurs only at sufficiently higher

temperatures than the desorption temperatures for most compounds. Measured T_{max} values can therefore be used as a fairly robust estimation for C^* of the respective composition. Thus, we performed calibration experiments, in order to establish the T_{max}-C^* relationship for both FIGAERO inlets used in this study (see Sect. ~~S3~~S5), and accordingly derived C^* for each measured organic composition from its respective T_{max} value. Note that in cases where thermogram peaks are affected by thermal decomposition (which we determined to play a relatively minor role in this study), we thereby implicitly assign upper-limit C^* values. We also note that relatively high collected aerosol mass (in the order of 1 µg) might induce so-called matrix effects in the evaporation process (Huang et al., 2018), which might in turn shift the observed T_{max} to higher temperatures, and could consequently lead to a slight systematic underestimation of C^*.

The results from the T_{max}-C^* conversion are shown in Fig. 6 and 7, summarizing them as Volatility Basis Sets (VBS) bins of one order of magnitude of C^*, as defined by Donahue et al., 2011 (SVOC = Semi-volatile Organic Compounds, green volatility range; LVOC = Low Volatility Organic Compounds, red volatility range; ELVOC = Extremely Low Volatility Organic Compounds, grey volatility range). These VBS distributions represent only the compounds found in the particle phase. Note that having translated from T_{max} to C^* using the instrument-specific calibration parameters, all results become comparable to each other. Also note that the abundance of SVOC compounds might generally be underestimated due to the fast evaporation of particulate matter during collection to FIGAERO filter and switching from collection phase to desorption phase.

A clear shift from higher to lower volatility for α-pinene SOA is observed with increasing OH exposure (Fig. 6). This shift manifests itself in the ~~disappearance~~ reduction of SVOC compounds while ~~especially~~ the amount of LVOC compounds increases. For sesquiterpene mixture SOA particles, a major part of the observed compounds falls into the LVOC class, while SVOC class compounds are almost non-existen~~ting~~. This is also seen in the α-pinene reference experiment, where most of the compounds are attributed to a single VBS bin. Note also the different y-scale in the α-pinene reference results compared to other results. A small number of signals in the sesquiterpene mixture results can confidently be categorized as thermal decomposition products, namely the ones that fall in the ELVOC volatility range but have relatively small molecular masses (< 200 Da). These compounds are C3-C7 compounds with relatively high oxygen content (O3-O7) and comprise about 11% of the total integrated signal.

In the Scots pine results (Fig. 7), a similar shift from higher to lower volatilities can be seen, with the Scots pine experiment 4 having the lowest volatility overall. Differences in the Scots pine VBS are probably due to evolving VOC emissions from the sapling. Note that simple SQT/MT ratio calculated from total amount of monoterpenes and sesquiterpenes (Table 1, insets in Fig. 8 top row) cannot explain the change in the volatility.

Finally, we examine the compositional information present in the FIGAERO datasets. In Fig. 8, we plot the carbon numbers versus oxygen numbers for each compound for each experiment, coloured according to the T_{max}-derived saturation concentration (C^*). The panels reveal the spread of compounds across the ranges of O:C ratios. In the α-pinene and sesquiterpene mixture experiments, the compounds fall roughly into similar areas (i.e., range of O:C ratios: 0.5 – 1.0), but in the Scots pine experiments the spread across different O:C ratios is notably wider. Specifically, there is an increased contribution of both relatively small (#C ~ 5) but highly oxygenated compounds and larger (C>10) though less oxygenated compounds (O:C < 0.5), both with relatively low effective volatility. This suggests that the bulk O:C ratio is insufficient to compare the expected properties of SOA particles generated from mixtures of different VOC precursors (e.g. MT and SQT, cf. average O:C and OSc values with standard deviations in Table 3.) Partially, the profoundly different spread of O:C ratios in the Scots pine experiment results might also be due to more extensive thermal fragmentation in the FIGAERO desorption process.

4. Summary and conclusions

In this study, we compared the physicochemical properties of SOA particles generated from combined ozonolysis and photo-oxidation of (1) α-pinene, (2) a complex mixture of VOCs emitted from Scots pine saplings, and (3) a mixture of farnesenes and bisabolenes which were ~~identified~~ observed to contribute a significant fraction to the Scots pine emissions. Our measurements examined the SOA mass yield, as well as the chemical composition and the thermal desorption properties of SOA particulate constituents to assess their volatility. In general, we found that all of these quantities or properties are substantially controlled by the ~~amount of OH exposure~~oxidative strength, as expected, but crucially also by the identity of the isomers making up the precursor VOC mixture.

The SOA mass yield from Scots pine emissions was in general lower than the SOA yield from α-pinene. The notable exception is a single experiment (Scots pine experiment 4) in which plant emissions were not dominated by farnesene and sesquiterpenes with similar structure, but by β-phellandrene and other monoterpenes. That experiment had the highest SOA yields among the Scots pine experiments, which is consistent with the high yields for the specifically involved monoterpenes reported or suggested in the literature (e.g. Faiola et al., 2018). For the other Scots pine experiments (experiments 1-3), we attribute the low observed SOA yields to the substantial contribution of acyclic sesquiterpenes, particularly β- and α-farnesene, to the total terpenoid plant emissions in those cases, ranging from 40-70% by mass. This is supported by our additional experiments that resulted in a much lower SOA yield from a mixture of mono and acyclic sesquiterpenes than from α-pinene. ~~When such acyclic compounds are oxidized, the initial reaction with OH or O_3 already leads to fragmentation (i.e. reaction products with much shorter C chain), whereas cyclic compounds, such as many monoterpenes, (including α-pinene and β-phellandrene) but also bicyclic sesquiterpenes (such as β-caryophyllene), generally go through more steps of~~

~~oxidation before the onset of significant fragmentation is observed. Such enhancement of the fragmentation processes~~The fragmentation of acyclic sesquiterpenes likely results in a product distribution containing a smaller amount of organic materials with sufficient low volatility to partition from the gas to particle phase. These acyclic sesquiterpenes might also go through multiple cycles of auto-oxidation following the reaction with OH, before suffering substantial fragmentation (Bianchi et al., 2019), which would explain the relatively high (>5) amount of oxygen atoms in a major fraction of the SOA compositions.

Indeed, our thermal desorption results indicate that the oxidation of acyclic and monocyclic sesquiterpenes forms a substantial amount of relatively small compounds, compared to α-pinene (Fig. 4). The average molecular weight of particle-phase α-pinene oxidation products decreases with increasing OH exposure (Table 3), while their O:C ratio increases. At the same time, the thermal desorption temperature of the SOA particulate constituents increased (Figs. 5-6), indicating a decrease in the effective SOA particle volatility.

Interestingly, our measurements showed that our Scots pine and sesquiterpene SOA particles were of lower volatility than any of the α-pinene SOA particles (even at higher oxidation exposure and comparable O:C/OS_C values). This result is indicated by both sum thermograms and supported by their derived VBS distributions for the individual SOA particulate constituents. It is also worth noting that, for the Scots pine experiments, the lowest-volatility SOA is formed in the experiment resulting in the highest SOA yields (Scots pine experiment 4), contrary to the observations made for the α-pinene experiments.

The molecular composition and thermal desorption behaviour of SOA particles observed with the FIGAERO instruments in ~~that~~ experiment 4 were strikingly similar to the other, sesquiterpene-dominated, Scots pine experiments 1-3. It appears that a certain contribution of those acyclic sesquiterpenes was~~is~~ sufficient to lower SOA volatility, whereas the monoterpenes that dominated the mixture led to the efficient formation of SOA to start with. Interestingly though, the monoterpenes did not seem to directly affect the volatility of Scots pine SOA, at least for our experiments here, even though their relative contribution to the precursor VOC mixture varied substantially. Further experiments are clearly warranted to explore this suggestion for a wider range of conditions and precursor mixtures than covered by this study.

In conclusion, our results highlight the need of knowing the structural identity of mixtures of VOCs, as typically encountered in real atmospheric conditions, if one endeavours an accurate prediction of SOA yields and SOA particle properties. In particular the emissions of sesquiterpenes need to be considered more carefully in current atmospheric models. Importantly, their effects on SOA yields can be both enhancing and suppressing, depending on the involved isomers. Specifically, depending on which sesquiterpene isomers are involved, the product distributions obtained from their oxidation can differ substantially from each other in terms of the products volatility and of the subsequent SOA chemistry. At the very least, a

differentiation between cyclic and acyclic terpenes is desirable. This issue is likely to become more relevant in the future, when biological and abiotic plant stressed events increase in frequency as is projected for a warming climate (Bale et al., 2002; Jactel et al., 2019). Such stresses will both increase biogenic VOC emissions and change the composition of emitted mixtures (Faiola et al., 2018, 2019).

Data availability. The data shown in the paper is available on request from corresponding author.

Author contributions. AV, CF, AB and TY-J designed the study. AY, AB, ZL, LB, AL, CF, EK and SN performed the measurements. AY and SS led the paper writing and all of the co-authors participated to the interpretation of the results and paper editing.

Competing interests. The authors declare that they have no conflict of interest.

Acknowledgements. The authors wish to thank James Blande, Minna Kivimäenpää and Rajendra Ghimire (University of Eastern Finland, Department of Environmental and Biological Science) for tending the Scots pine seedlings. Sergey A. Nizkorodov acknowledges the Fulbright Finland Foundation and the Saastamoinen Foundation that funded his visit to the University of Eastern Finland.

Financial support. This research was supported by Academy of Finland (272041, 310682, 299544), European Research Council (ERC-StQ QAPPA 335478) and University of Eastern Finland Doctoral Program in Environmental Physics, Health and Biology.

References

Amin, H., Atkins, P. T., Russo, R. S., Brown, A. W., Sive, B., Hallar, A. G. and Huff Hartz, K. E.: Effect of Bark Beetle Infestation on Secondary Organic Aerosol Precursor Emissions, Environ. Sci. Technol., 46(11), 5696–5703, doi:10.1021/es204205m, 2012.

Bäck, J., Aalto, J., Henriksson, M., Hakola, H., He, Q. and Boy, M.: Chemodiversity of a Scots pine stand and implications for terpene air concentrations, Biogeosciences, 9(2), 689–702, doi:10.5194/bg-9-689-2012, 2012.

Bale, J. S., Masters, G. J., Hodkinson, I. A. N. D., Awmack, C., Bezemer, T. M., Brown, V. K., Butterfield, J., Buse, A.,

Coulson, J. C., Farrar, J., Good, J. E. G., Harrington, R., Hartley, S., Jones, T. H., Lindroth, R. L. and Press, M. C.: Herbivory in global climate change research : direct effects of rising temperature on insect herbivores, 2002.

Bannan, T. J., Le Breton, M., Priestley, M., Worrall, S. D., Bacak, A., Marsden, N. A., Merha, A., Hammes, J., Hallquist, M., Alfarra, M. R., Krieger, U. K., Reid, J. P., Jayne, J., Robinson, W., McFiggans, G., Coe, H., Percival, C. J. and Topping, D.: A method for extracting calibrated volatility information from the FIGAERO-HR-ToF-CIMS and its application to chamber and field studies, , (August), 1–12, doi:10.5194/amt-2018-255, 2018.

Berg, A. R., Heald, C. L., Huff Hartz, K. E., Hallar, A. G., Meddens, A. J. H., Hicke, J. A., Lamarque, J.-F. and Tilmes, S.: The impact of bark beetle infestations on monoterpene emissions and secondary organic aerosol formation in western North America, Atmos. Chem. Phys., 13(6), 3149–3161, doi:10.5194/acp-13-3149-2013, 2013.

Bianchi, F., Kurten, T., Riva, M., Mohr, C., Rissanen, M. P., Roldin, P., Berndt, T., Crounse, J. D., Wennberg, P. O., Mentel, T. F., Wildt, J., Junninen, H., Jokinen, T., Kulmala, M., Worsnop, D. R., Thornton, J. A., Donahue, N., Kjaergaard, H. G. and Ehn, M.: Highly Oxygenated Organic Molecules (HOM) from Gas-Phase Autoxidation Involving Peroxy Radicals : A Key Contributor to Atmospheric Aerosol, , doi:10.1021/acs.chemrev.8b00395, 2019.

Blande, J. D., Turunen, K. and Holopainen, J. K.: Pine weevil feeding on Norway spruce bark has a stronger impact on needle VOC emissions than enhanced ultraviolet-B radiation, Environ. Pollut., 157(1), 174–180, doi:10.1016/J.ENVPOL.2008.07.007, 2009.

Buchholz, A., Lambe, A. T., Ylisirniö, A., Li, Z., Tikkanen, O., Faiola, C., Kari, E., Hao, L., Luoma, O., Huang, W., Mohr, C., Worsnop, D. R. and Nizkorodov, S. A.: Insights into the O : C-dependent mechanisms controlling the evaporation of α -pinene secondary organic aerosol particles, , 4061–4073, 2019.

Capouet, M. and Müller, J.-F.: A group contribution method for estimating the vapour pressures of α-pinene oxidation products, Atmos. Chem. Phys., 6(6), 1455–1467, doi:10.5194/acp-6-1455-2006, 2006.

Donahue, N. M., Epstein, S. A., Pandis, S. N. and Robinson, A. L.: A two-dimensional volatility basis set: 1. organic-aerosol mixing thermodynamics, Atmos. Chem. Phys., 11(7), 3303–3318, doi:10.5194/acp-11-3303-2011, 2011.

Faiola, C. L., Buchholz, A., Kari, E., Yli-Pirilä, P., Holopainen, J. K., Kivimäenpää, M., Miettinen, P., Worsnop, D. R., Lehtinen, K. E. J., Guenther, A. B. and Virtanen, A.: Terpene Composition Complexity Controls Secondary Organic Aerosol Yields from Scots Pine Volatile Emissions, Sci. Rep., 8(1), 1–13, doi:10.1038/s41598-018-21045-1, 2018.

Faiola, C. L., Pullinen, I., Buchholz, A., Khalaj, F., Ylisirnio, A., Kari, E., Schobesberger, S., Yli-juuti, T., Miettinen, P., Holopainen, J. K. and Kivima, M.: Secondary Organic Aerosol Formation from Healthy and Aphid- Stressed Scots Pine Emissions, , doi:10.1021/acsearthspacechem.9b00118, 2019.

Hall, W. A., Pennington, M. R. and Johnston, M. V.: Molecular transformations accompanying the aging of laboratory secondary organic aerosol, Environ. Sci. Technol., 47(5), 2230–2237, doi:10.1021/es303891q, 2013.

Hellén, H., Praplan, A. P., Tykkä, T., Ylivinkka, I., Vakkari, V., Bäck, J., Petäjä, T., Kulmala, M. and Hakola, H.: Long-term measurements of volatile organic compounds highlight the importance of sesquiterpenes for the atmospheric chemistry of a boreal forest, Atmos. Chem. Phys., 18(19), 13839–13863, doi:10.5194/acp-18-13839-2018, 2018.

Holopainen, J. K. and Gershenzon, J.: Multiple stress factors and the emission of plant VOCs, Trends Plant Sci., 15(3), 176–184, doi:10.1016/j.tplants.2010.01.006, 2010.

Holopainen, J. K., Kivimäenpää, M. and Nizkorodov, S. A.: Plant-derived Secondary Organic Material in the Air and Ecosystems, Trends Plant Sci., 22(9), 744–753, doi:10.1016/j.tplants.2017.07.004, 2017.

Huang, W., Saathoff, H., Pajunoja, A., Shen, X., Naumann, K. and Wagner, R.: α -Pinene secondary organic aerosol at low temperature : chemical composition and implications for particle viscosity, , 2883–2898, 2018.

Iyer, S., He, X., Hyttinen, N., Kurtén, T. and Rissanen, M. P.: Computational and Experimental Investigation of the Detection of HO_2 Radical and the Products of Its Reaction with Cyclohexene Ozonolysis Derived RO_2 Radicals by an Iodide-Based Chemical Ionization Mass Spectrometer, J. Phys. Chem. A, 121(36), 6778–6789, doi:10.1021/acs.jpca.7b01588, 2017.

Jactel, H., Koricheva, J. and Castagneyrol, B.: ScienceDirect Responses of forest insect pests to climate change : not so simple, , doi:10.1016/j.cois.2019.07.010, 2019.

Jaoui, M., Leungsakul, S. and Kamens, R. M.: Gas and Particle Products Distribution from the Reaction of β -Caryophyllene with Ozone, , 261–287, 2003.

Jaoui, M., Kleindienst, T. E., Docherty, K. S., Lewandowski, M. and Offenberg, J. H.: Secondary organic aerosol formation from the oxidation of a series of sesquiterpenes: α-cedrene, β-caryophyllene, α-humulene and α-farnesene with O_3, OH and NO_3 radicals, Environ. Chem., 10(3), 178, doi:10.1071/EN13025, 2013.

Kari, E., Miettinen, P., Yli-Pirilä, P., Virtanen, A. and Faiola, C. L.: PTR-ToF-MS product ion distributions and humidity-dependence of biogenic volatile organic compounds, Int. J. Mass Spectrom., 430, 87–97, doi:10.1016/j.ijms.2018.05.003, 2018.

Kourtchev, I., Bejan, I., Sodeau, J. R. and Wenger, J. C.: Gas-phase reaction of (E)-β-farnesene with ozone: Rate coefficient and carbonyl products, Atmos. Environ., 43(20), 3182–3190, doi:10.1016/j.atmosenv.2009.03.048, 2009.

Kourtchev, I., Bejan, I., Sodeau, J. R. and Wenger, J. C.: Gas phase reaction of OH radicals with (E)-β-farnesene at 296 ± 2 K: Rate coefficient and carbonyl products, Atmos. Environ., 46, 338–345, doi:10.1016/j.atmosenv.2011.09.061, 2012.

Krieger, U. K., Siegrist, F., Marcolli, C., Emanuelsson, E. U., Gøbel, F. M., Bilde, M., Marsh, A., Reid, J. P., Huisman, A. J., Riipinen, I., Hyttinen, N., Myllys, N., Kurtén, T., Bannan, T., Percival, C. J. and Topping, D.: A reference data set for validating vapor pressure measurement techniques : homologous series of polyethylene glycols, , 49–63, 2018.

Kroll, J. H., Donahue, N. M., Jimenez, J. L., Kessler, S. H., Canagaratna, M. R., Wilson, K. R., Altieri, K. E., Mazzoleni, L. R., Wozniak, A. S., Bluhm, H., Mysak, E. R., Smith, J. D., Kolb, C. E. and Worsnop, D. R.: Carbon oxidation state as a metric for describing the chemistry of atmospheric organic aerosol, Nat. Chem., 3(2), 133–139, doi:10.1038/nchem.948, 2011.

Lambe, A. T., Onasch, T. B., Croasdale, D. R., Wright, J. P., Martin, A. T., Franklin, J. P., Massoli, P., Kroll, J. H., Canagaratna, M. R., Brune, W. H., Worsnop, D. R. and Davidovits, P.: Transitions from Functionalization to Fragmentation

Reactions of Laboratory Secondary Organic Aerosol (SOA) Generated from the OH Oxidation of Alkane Precursors, Environ. Sci. Technol., 46(10), 5430–5437, doi:10.1021/es300274t, 2012.

Lee, A., Goldstein, A. H., Kroll, J. H., Ng, N. L., Varutbangkul, V., Flagan, R. C. and Seinfeld, J. H.: Gas-phase products and secondary aerosol yields from the photooxidation of 16 different terpenes, J. Geophys. Res., 111(D17), D17305, doi:10.1029/2006JD007050, 2006.

Lee, B. H., Lopez-Hilfiker, F. D., Mohr, C., Kurtén, T., Worsnop, D. R. and Thornton, J. A.: An Iodide-Adduct High-Resolution Time-of-Flight Chemical-Ionization Mass Spectrometer: Application to Atmospheric Inorganic and Organic Compounds, Environ. Sci. Technol., 48(11), 6309–6317, doi:10.1021/es500362a, 2014.

Lopez-Hilfiker, F. D., Mohr, C., Ehn, M., Rubach, F., Kleist, E., Wildt, J., Mentel, T. F., Lutz, A., Hallquist, M., Worsnop, D. and Thornton, J. A.: A novel method for online analysis of gas and particle composition: Description and evaluation of a filter inlet for gases and AEROsols (FIGAERO), Atmos. Meas. Tech., 7(4), 983–1001, doi:10.5194/amt-7-983-2014, 2014.

Lopez-Hilfiker, F. D., Mohr, C., Ehn, M., Rubach, F., Kleist, E., Wildt, J., Mentel, T. F., Carrasquillo, a. J., Daumit, K. E., Hunter, J. F., Kroll, J. H., Worsnop, D. R. and Thornton, J. a.: Phase partitioning and volatility of secondary organic aerosol components formed from α-pinene ozonolysis and OH oxidation: the importance of accretion products and other low volatility compounds, Atmos. Chem. Phys., 15, 7765–7776, doi:10.5194/acp-15-7765-2015, 2015.

Mackenzie-Rae, F. A., Liu, T., Deng, W., Saunders, S. M., Fang, Z., Zhang, Y. and Wang, X.: Ozonolysis of α-phellandrene – Part 1: Gas- and particle-phase characterisation, Atmos. Chem. Phys., 17(11), 6583–6609, doi:10.5194/acp-17-6583-2017, 2017.

McFiggans, G., Mentel, T. F., Wildt, J., Pullinen, I., Kang, S., Kleist, E., Schmitt, S., Springer, M., Tillmann, R., Wu, C., Zhao, D., Hallquist, M., Faxon, C., Breton, M. Le, Hallquist, A. M., Simpson, D., Bergstro, R., Jenkin, M. E., Ehn, M., Thornton, J. A., Alfarra, M. R., Bannan, T. J., Percival, C. J., Priestley, M., Topping, D. and Kiendler-scharr, A.: Secondary organic aerosol reduced by mixture of atmospheric vapours, Nature, 0–6, doi:10.1038/s41586-018-0871-y, 2019.

Ng, N. L., Brown, S. S., Archibald, A. T., Atlas, E., Cohen, R. C., Crowley, J. N., Day, D. A., Donahue, N. M., Fry, J. L., Fuchs, H., Griffin, R. J., Guzman, M. I., Herrmann, H., Hodzic, A., Iinuma, Y., Kiendler-Scharr, A., Lee, B. H., Luecken, D. J., Mao, J., McLaren, R., Mutzel, A., Osthoff, H. D., Ouyang, B., Picquet-Varrault, B., Platt, U., Pye, H. O. T., Rudich, Y., Schwantes, R. H., Shiraiwa, M., Stutz, J., Thornton, J. A., Tilgner, A., Williams, B. J. and Zaveri, R. A.: Nitrate radicals and biogenic volatile organic compounds: Oxidation, mechanisms, and organic aerosol, Atmos. Chem. Phys., 17(3), 2103–2162, doi:10.5194/acp-17-2103-2017, 2017.

Odum Jay, R., Hoffmann, T., Bowman, F., Collins, D., Flagan Richard, C. and Seinfeld John, H.: Gas particle partitioning and secondary organic aerosol yields, Environ. Sci. Technol., 30(8), 2580–2585, doi:10.1021/es950943+, 1996.

Pankow, J. F. and Asher, W. E.: SIMPOL.1: A simple group contribution method for predicting vapor pressures and enthalpies of vaporization of multifunctional organic compounds, Atmos. Chem. Phys., 8(10), 2773–2796, doi:10.5194/acp-8-2773-2008, 2008.

Passananti, M., Zapadinsky, E., Zanca, T., Ehn, M., Attoui, M. and Vehkama, H.: ChemComm How well can we predict

cluster fragmentation, , 5946–5949, doi:10.1039/c9cc02896j, 2019.

Peng, Z., Day, D. A., Stark, H., Li, R., Lee-Taylor, J., Palm, B. B., Brune, W. H. and Jimenez, J. L.: HOx radical chemistry in oxidation flow reactors with low-pressure mercury lamps systematically examined by modeling, Atmos. Meas. Tech., 8(11), 4863–4890, doi:10.5194/amt-8-4863-2015, 2015.

Peng, Z., Day, D. A., Ortega, A. M., Palm, B. B., Hu, W., Stark, H., Li, R., Tsigaridis, K., Brune, W. H. and Jimenez, J. L.: Non-OH chemistry in oxidation flow reactors for the study of atmospheric chemistry systematically examined by modeling, Atmos. Chem. Phys., 16(7), 4283–4305, doi:10.5194/acp-16-4283-2016, 2016.

Schobesberger, S., D'Ambro, E. L., Lopez-Hilfiker, F. D., Mohr, C. and Thornton, J. A.: A model framework to retrieve thermodynamic and kinetic properties of organic aerosol from composition-resolved thermal desorption measurements, Atmos. Chem. Phys., 18(20), 14757–14785, doi:10.5194/acp-18-14757-2018, 2018.

Surratt, J. D., Gómez-González, Y., Chan, A. W. H., Vermeylen, R., Shahgholi, M., Kleindienst, T. E., Edney, E. O., Offenberg, J. H., Lewandowski, M., Jaoui, M., Maenhaut, W., Claeys, M., Flagan, R. C. and Seinfeld, J. H.: Organosulfate Formation in Biogenic Secondary Organic Aerosol, J. Phys. Chem. A, 112(36), 8345–8378, doi:10.1021/jp802310p, 2008.

Yassaa, N., Song, W., Lelieveld, J., Vanhatalo, A., Bäck, J. and Williams, J.: Diel cycles of isoprenoids in the emissions of Norway spruce, four Scots pine chemotypes, and in Boreal forest ambient air during HUMPPA-COPEC-2010, Atmos. Chem. Phys., 12(15), 7215–7229, doi:10.5194/acp-12-7215-2012, 2012.

635 **Table 1. List of different Scots pine experiments with corresponding PAM 1 reactor conditions. Monoterpenes are referred to as MT and sesquiterpenes as SQT. Collected mass is estimated from SMPS data assuming particle density of 1.3 g cm^{-3}.**

Experiment	**Scots pine 1**	**Scots pine 2**	**Scots pine 3**	**Scots pine 4**
VOC mixing ratio (ppb from PTR-ToF-MS)	MT: 125 ± 1 SQT: 179 ± 1 Sum: 304 ± 2	MT: 213 ± 14 SQT: 179 ± 1 Sum: 391 ± 14	MT: 127 ± 4 SQT: 151 ± 1 Sum: 278 ± 4	MT: 153 ± 3 SQT: 66 ± 2 Sum: 218 ± 3
SQT/MT-ratio (by molar ratio)	1.43	0.85	1.2	0.4
SQT/MT-ratio (by mass ratio)	2.15	1.26	1.78	0.65
OH-exposure (molecules $cm^{-3}s$)	6.41 x 10^{11}	6.49 x 10^{11}	6.45 x 10^{11}	7.31 x 10^{11}
PAM residence time (s)	300	300	300	300
O_3 mixing ratio (ppm)	4.9	5	5	5.6
Collected mass on FIGAERO filter (ng)	1000	1200	1300	1000

Table 2. List of different α-pinene and sesquiterpene experiments with corresponding PAM-reactor conditions. Collected mass is estimated from SMPS data assuming particle density of 1.3 g cm^{-3}

	PAM 1			**PAM 2**	
Experiment	**α-pinene low exposure**	**α-pinene medium exposure**	**α-pinene high exposure**	**Sesquiterpene mixture**	**α-pinene reference**
VOC mixing ratio (ppb from PTR-ToF-MS)	199 ± 2	198 ± 2	196 ± 2	327 ± 5	270 ± 10
OH-exposure (molecules cm^{-3} s)	2.54 x 10^{11}	6.85 x 10^{11}	2.45 x 10^{12}	8.2 x 10^{10}	2.6 x 10^{11}
PAM residence time (s)	120	120	120	160	160
O_3 mixing ratio (ppm)	6.6	25	25	13.3	13.2
Collected mass (ng)	960	880	1350	550	925

645 **Table 3. Average O:C ratio, OSc and chemical composition from each experiment calculated from AMS and FIGAERO data. Values calculated from FIGAERO are weighted by the integrated signal strength. All FIGAERO data is shown with standard deviation to highlight the spread of different compositions in the mass spectrum.**

Experiment	**<O:C> AMS**	**<O:C> FIGAERO**	**<OSc> AMS**	**<OSc> FIGAERO**	**<$C_xH_yO_z$>**
α-pinene low exposure	0.53	0.65±0.28	-0.46	-0.3±0.56	$C_{9\pm4}H_{14.2\pm4}O_{5.4\pm4}$
α-pinene medium exposure	0.69	0.75±0.3	-0.05	0.02±0.65	$C_{8.3\pm3.5}H_{12.1\pm3.5}O_{5.7\pm3.5}$
α-pinene high exposure	0.96	0.9±0.33	0.63	0.47±0.73	$C_{7.5\pm3}H_{9.9\pm4.5}O_{6\pm1.9}$
Scots pine experiment 1	0.85	0.79±0.43	0.37	0.02±1.1	$C_{8.5\pm4}H_{13.6\pm8}O_{5.4\pm2}$
Scots pine experiment 2	0.89	0.77±0.42	0.43	-0.04±1.1	$C_{8.4\pm4}H_{13.5\pm8.3}O_{5.4\pm2.1}$
Scots pine experiment 3	0.9	0.79±0.43	0.55	0.02±1.1	$C_{8.7\pm4}H_{14\pm7.9}O_{5.4\pm2.1}$
Scots pine experiment 4	1	0.81±0.43	0.75	0.06±1.1	$C_{8.2\pm3.7}H_{13.1\pm7.5}O_{5.3\pm2}$
Sesquiterpene mixture	0.82	0.89±0.37	0.26	0.47±0.83	$C_{7.5\pm3.7}H_{9.7\pm5.1}O_{5.6\pm1.8}$
α-pinene reference	0.77	0.82±0.33	0.06	0.28±0.71	$C_{7.4\pm3}H_{10\pm4.4}O_{5.3\pm1.5}$

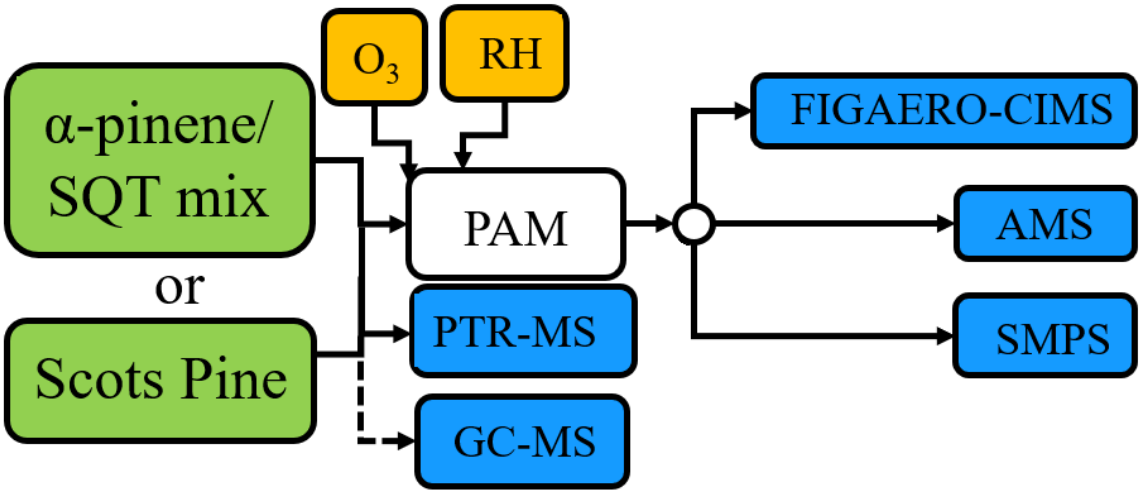

650

Figure 1: Measurement setup used in the experiments. Abbreviations in the picture are explained in the main text (Sect. 2), except for ozone-containing air (O_3) and humidified air (RH).

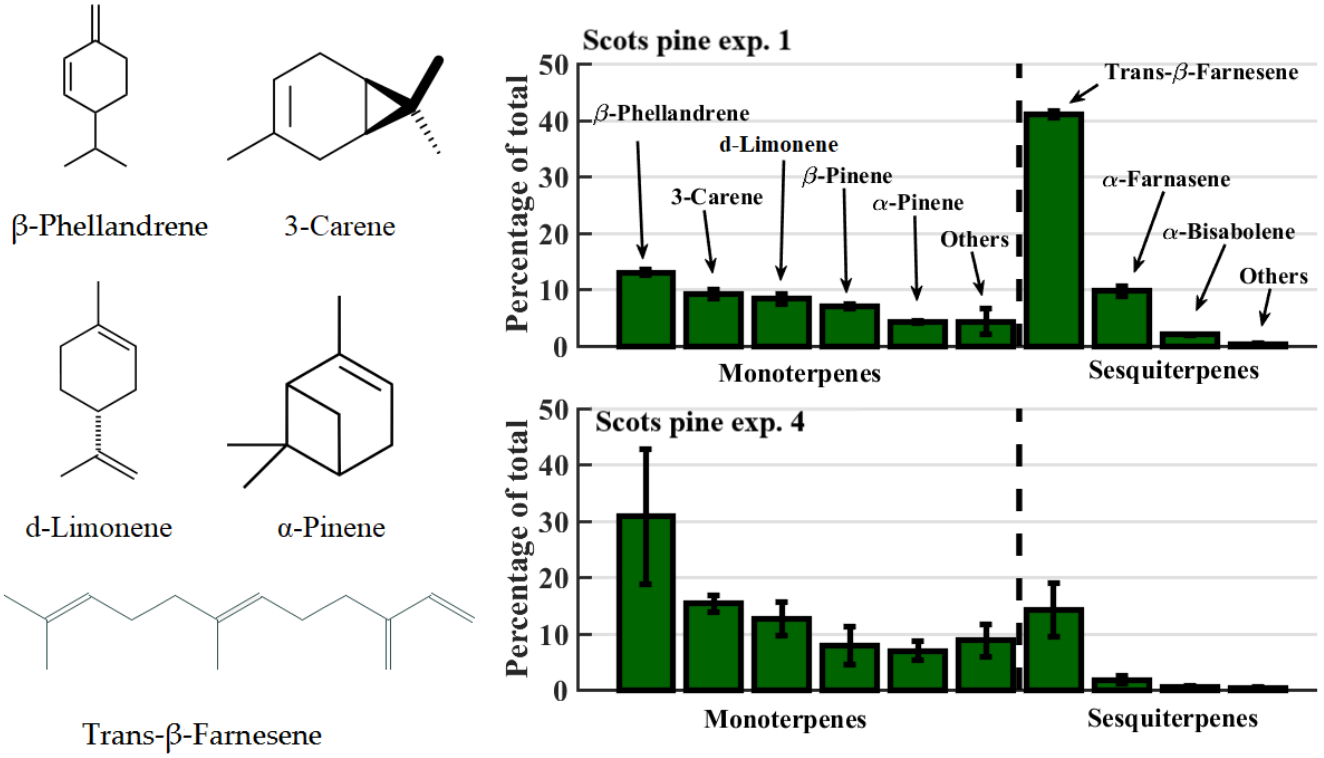

Figure 2: Left panel shows the structures of the most abundant monoterpenes and sesquiterpenes in Scots pine emissions, as measured with TD-GC-MS. Relative mass concentrations of each compound are shown in the right panel for Scots pine experiments 1 (top) and 4 (bottom), the latter following deliberate damage to the plant's stem. The whiskers show the standard deviation of the measurements.

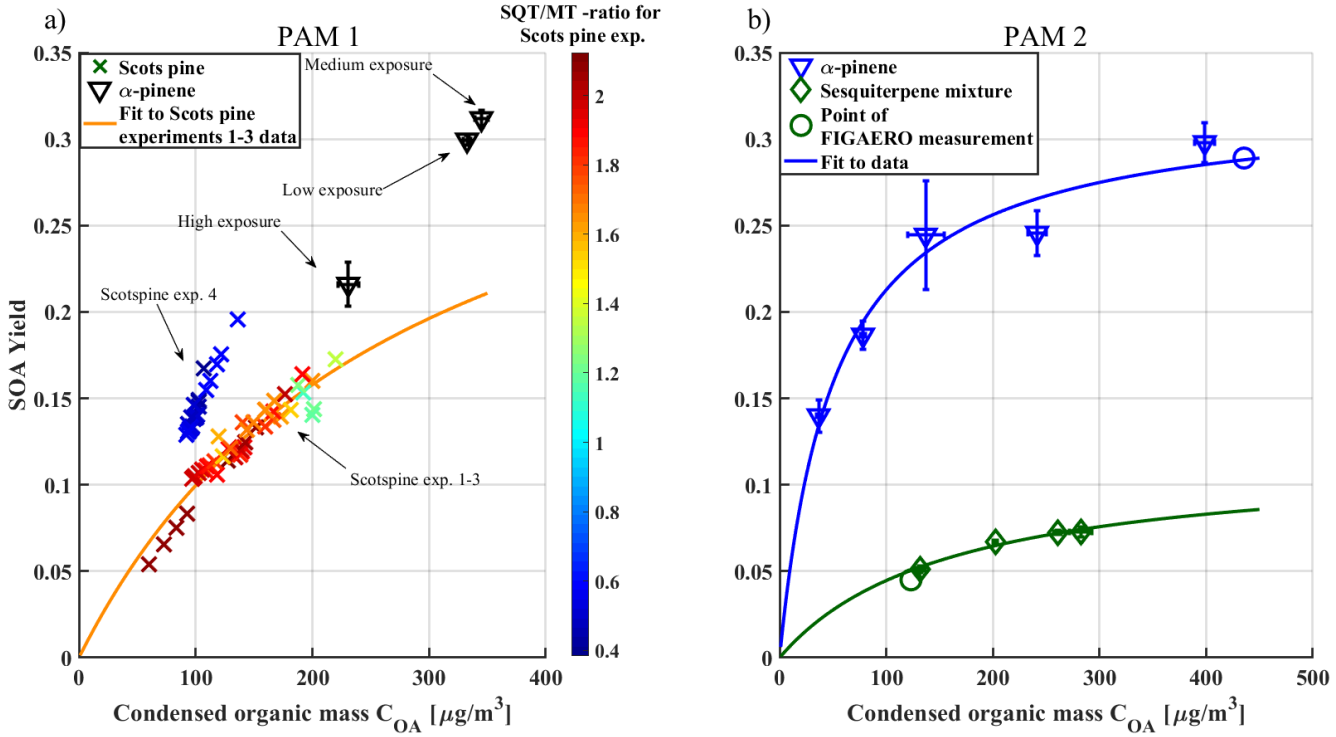

Figure 3: Panel a) SOA yield vs. Condensed organic mass (C_{oa}) from Scots pine and α-pinene experiments. Each point represents a single SMPS scan. In these cases, and error bars are omitted for clarity. The color scale on the Scots pine experiment results corresponds to the sesquiterpene-to-monoterpene (SQT/MT) ratio by mass ratio (crosses; showing all yield measurements, reflecting the variability in plant emission rates). Each α-pinene experiment is averaged to one point (black triangles) and labelled. Error bars shown are standard deviations of multiple scans. The orange curve is fit with equation (2) to the Scots pine experiments 1-3 (SQT/MT > 1) with fit parameters: $\alpha_1 = 0.3783$, $K_1 = 0.0035$, $\alpha_2 = 0.0029$ and $K_2 = 0.0035$. Panel b) α-pinene reference and sesquiterpene mixture SOA yields versus C_{OA} and Odum fits to both datasets. The fit parameters are for α-pinene: $\alpha_1 = 0.3219$, $K_1 = 0.0195$ and for the sesquiterpene mixture: $\alpha_1 = 0.1164$, $K_1 = 0.0062$. Circles shows the points of FIGAERO measurements. Titles "PAM 1" (panel a) and "PAM 2" (panel b) refer to different PAM reactors used in the experiments.

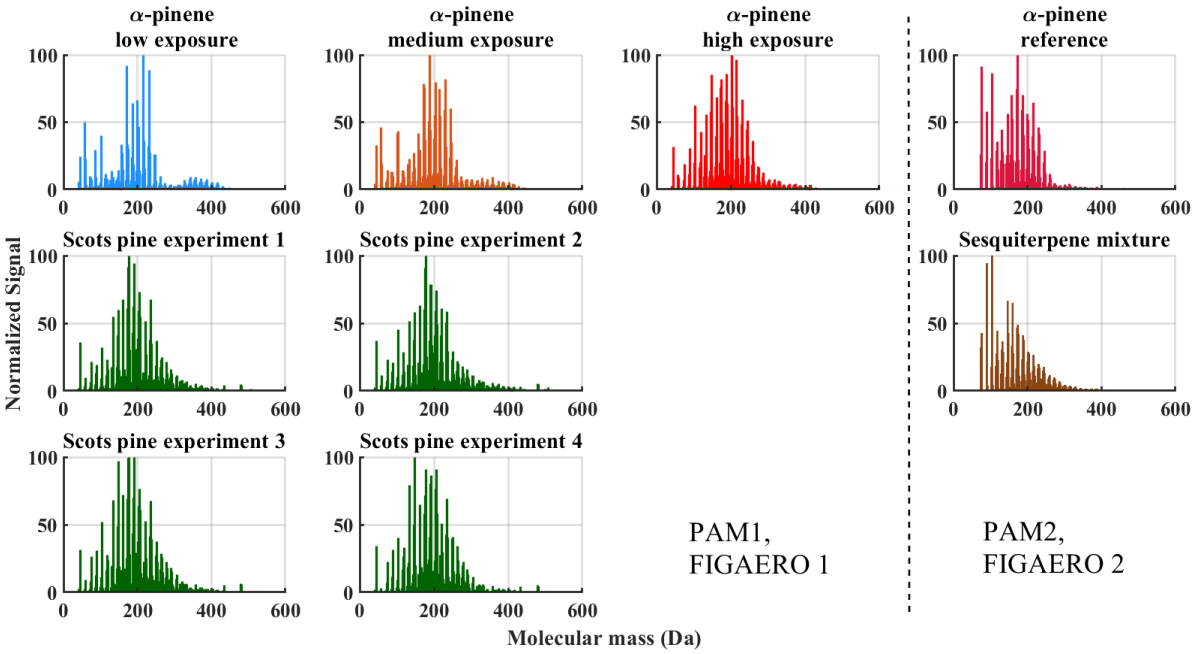

Figure 4: Mass spectra integrated over the whole FIGAERO desorption cycle for each experiment. Each spectrum is normalized to the peak height of the most abundant ion.

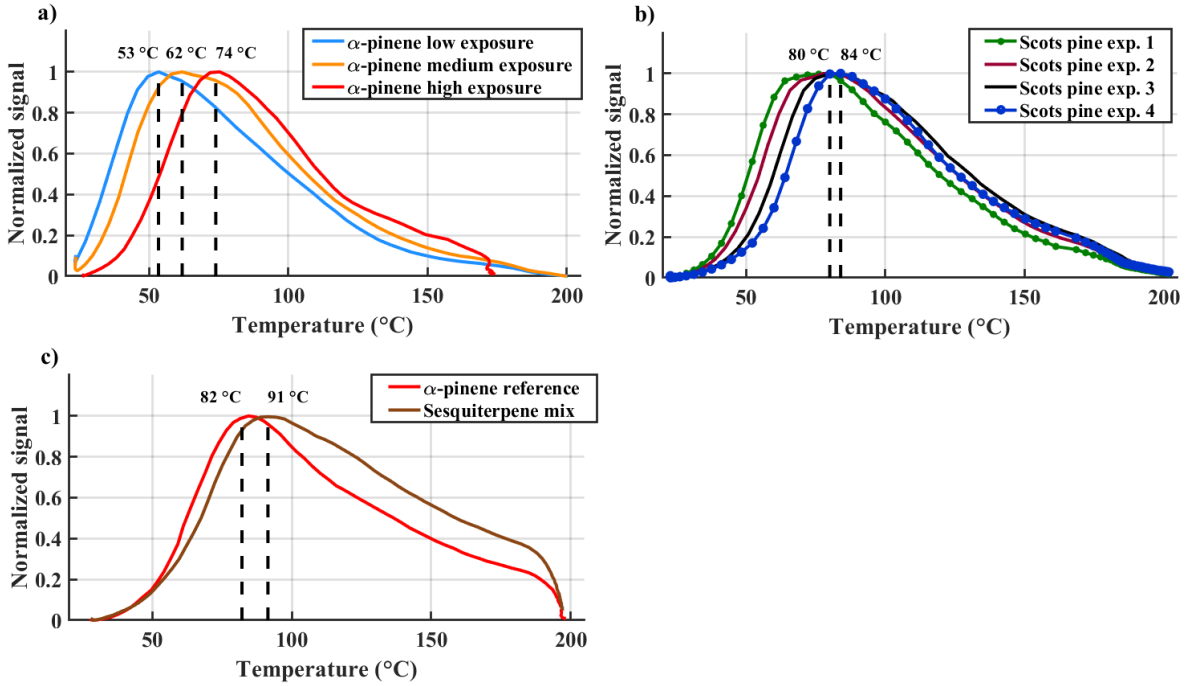

675

Figure 5: Normalized sum thermograms (all observed ions containing C, H, and O atoms) from a) α-pinene experiments, b) Scots pine experiments 1 - 4 and c) sesquiterpene mixture experiment, together with reference α-pinene experiment. T_{max} values of the sum thermograms are shown with dashed lines. In panel b) T_{max} values of only Scots pine experiment 1 and Scots pine experiment 4 are shown for clarity.

680

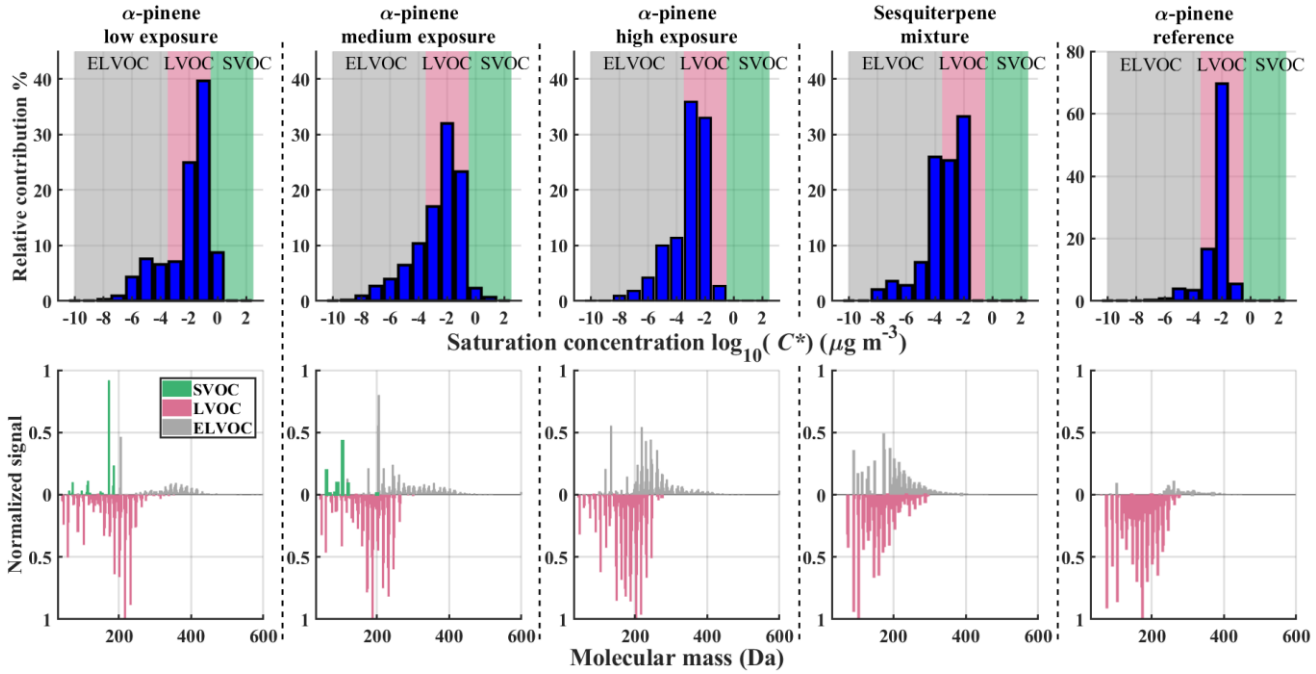

Figure 6: VBS bins and corresponding normalized integrated mass spectra from α-pinene low, medium and high experiment, sesquiterpene mixture, and α-pinene reference experiment. Top row: VBS bins determined from *Tmax* with background colours corresponding to different volatility classes (defined in the text). Bottom row: Integrated FIGAERO signal normalized to maximum signal and coloured by corresponding volatility class. LVOC class compounds (red) are plotted on an inverted y-axis for easier distinction from other volatility classes VBS.

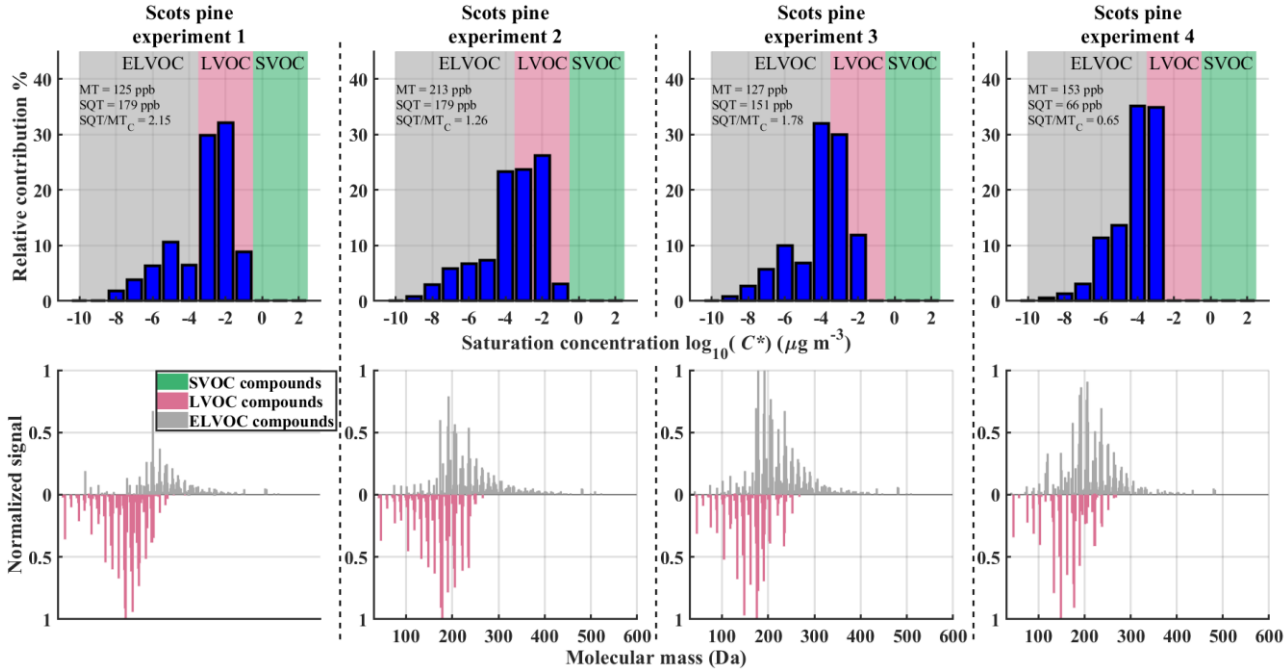

Figure 7: VBS bins and corresponding normalized integrated mass spectra in the Scots pine experiments. Top row: VBS bins determined from T_{max} with background colours corresponding to different volatility classes. Bottom row: Integrated FIGAERO signal normalized to maximum signal coloured by corresponding volatility class. LVOC class is plotted on reverse y-axis for easier distinction from other volatility classes. Text in the upper row panels show measured amounts of monoterpenes and sesquiterpenes and calculated SQT/MT ratio per mass ratio.

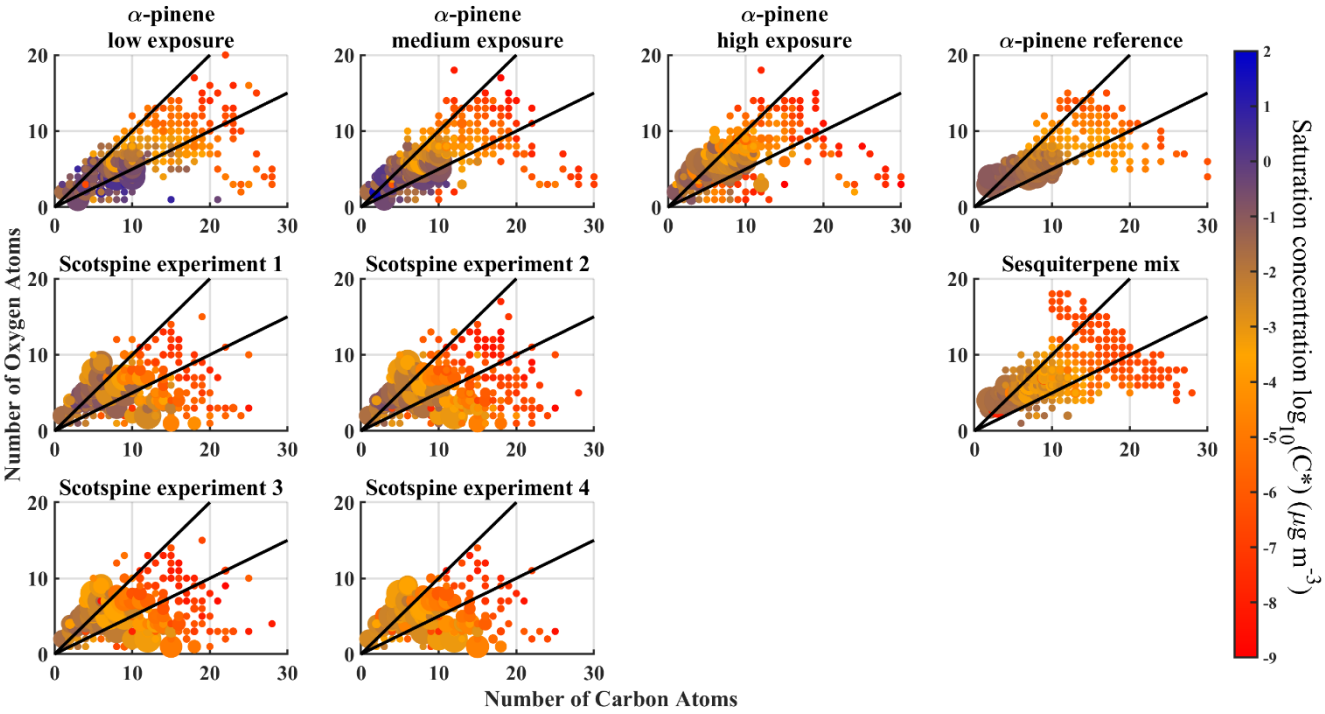

695

Figure 8: Number of oxygen molecules versus number of carbon molecules for each compound and each experiment. Colours correspond to the saturation ratio *C as derived from the measured T_{max}. The size of a marker corresponds to the signal of the compound. The two black lines in the figures correspond to O:C = 0.5 and O:C = 1 ratios, for reference.**

700